Front. Earth Sci. 2023, 17(1): 197–217
https://doi.org/10.1007/s11707-022-1000-7

RESEARCH ARTICLE

Critical tectonic events and their geological controls on deep buried coalbed methane accumulation in Daning-Jixian Block, eastern Ordos Basin

Taotao YAN (✉)[1,2], Shan HE[3], Shuai ZHENG[4], Yadong BAI[5], Wei CHEN[6], Yanjun MENG[1], Shangwen JIN[1], Huifang YAO[1], Xiaobao JIA[7]

1 College of Mining Engineering, Taiyuan University of Technology, Taiyuan 030024, China
2 Coal Reservoir Laboratory of National Engineering Research Center of CBM Development & Utilization, China University of Geosciences, Beijing 100083, China
3 Shanxi CBM Exploration and Development Branch, PetroChina Huabei Oilfield Company, Changzhi 046000, China
4 China Coal Geology Group Co., Ltd, Beijing 100083, China
5 Research Institute of Petroleum Exploration and Development-Northwest, PetroChina, Lanzhou 730000, China
6 Beijing Furuibao Energy Technology Company, Beijing 100176, China
7 Shanxi Province 148 Ecological Geology Technology Co., Ltd, Taiyuan 030053, China

Abstract Commercial exploration and development of deep buried coalbed methane (CBM) in Daning-Jixian Block, eastern margin of Ordos Basin, have rapidly increased in recent decades. Gas content, saturation and well productivity show significant heterogeneity in this area. To better understand the geological controlling mechanism on gas distribution heterogeneity, the burial history, hydrocarbon generation history and tectonic evolution history were studied by numerical simulation and experimental simulation, which could provide guidance for further development of CBM in this area. The burial history of coal reservoir can be classified into six stages, i.e., shallowly buried stage, deeply burial stage, uplifting stage, short-term tectonic subsidence stage, large-scale uplifting stage, sustaining uplifting and structural inversion stage. The organic matter in coal reservoir experienced twice hydrocarbon generation. Primary and secondary hydrocarbon generation processes were formed by the Early and Middle Triassic plutonic metamorphism and Early Cretaceous regional magmatic thermal metamorphism, respectively. Five critical tectonic events of the Indosinian, Yanshanian and Himalayan orogenies affect different stages of the CBM reservoir accumulation process. The Indosinian orogeny mainly controls the primary CBM generation. The Yanshanian Orogeny dominates the second gas generation and migration processes. The Himalayan orogeny mainly affects the gas dissipation process and current CBM distribution heterogeneity.

Received March 31, 2022; accepted June 5, 2022

E-mail: taotao87225@163.com

Keywords deep buried coalbed methane, coal reservoir accumulation evolution, numerical simulation, Daning-Jixian Block

1 Introduction

With the decrease of new proven available reserves in shallow buried areas, the exploration and development technologies of deep buried coalbed methane (CBM) have become a hot topic in recent years (Qin and Shen, 2016). The areas that conduct commercial development of deep buried CBM resources in China mainly distributed in the eastern margin of Ordos Basin (e.g., Yanchuannan and Daning-Jixian Blocks) and Qinshui Basin (e.g., Zheng-zhuang and Shizhuang Blocks) (Li et al., 2016). Among these blocks, Daning-Jixian Block is one of the most important areas for the co-exploration and co-exploitation of coal measure gas (CMG). The proved resources of deep buried CBM and tight sandstone gas in this area is about 148.3 billion m^3 and 70.9 billion m^3, respectively, which shows great economic developmental potential (Li et al., 2011). Many research works have been carried out in Daning-Jixian Block for deep buried CBM reservoir exploration, including distribution characteristics of CBM (Sun et al., 2004), sedimentary environment analysis (Sun and Wang, 2006), *in situ* stress field characteristics (Jiang et al., 2016), analysis on origin types of CBM (Chao and Wang, 2016; Mu et al., 2016), production characteristics of deep buried CBM (Huang et al., 2018; Nie et al., 2018;

Nie et al., 2022), favorable area evaluation (Yan et al., 2021a; Li et al., 2022), and qualitative research on CBM accumulation (Li et al., 2022). However, to the best of the authors' knowledge, effective research on the coal reservoir evolution and CBM accumulation process has not been conducted in this area.

The evolution of CBM reservoir is a complex dynamic process that includes coal organic matter maturation and gas generation processes (Scott et al., 1994; Boreham et al., 1998; Johnson and Flores, 1998; Wu et al., 2000; Payne and Ortoleva, 2001), as well as the gas sorption, migration, diffusion, pooling and accumulation processes (Scott, 2002; Yao et al., 2009; Cai et al., 2011; Karacan and Goodman, 2012; Song et al., 2012; Vishal et al., 2015; Xu et al., 2015). The comprehensive analysis and restoration of these dynamic processes is critical for the understanding of gas enrichment characteristics in coal reservoir. Basin-scale investigations on the CBM reservoir formation history have been performed by many scholars in different sedimentary basins (Boreham et al., 1998; Johnson and Flores, 1998; Payne and Ortoleva, 2001; Faiz et al., 2007; Wei et al., 2007, 2008, 2010; Alsaab et al., 2009; Sachsenhofer et al., 2012; Cai et al., 2014; Yan et al., 2015, 2021b).

In this research, the burial history, geothermal evolution history and hydrocarbon generation history of deep buried CBM reservoir in Daning-Jixian Block were simulated for clarification of the geological control effects on the dynamic processes of CBM accumulation and the enrichment characteristic of current gas in different tectonic domains. The research results have a crucial significance for exploration and development of deep CBM in this area.

2 Geological settings

Daning-Jixian Block located in the eastern margin of Ordos Basin. The structural contour map of the No. 8 coal seam is shown in Fig. 1. Tectonically, the Daning-Jixian Block is a monocline which inclines to west (Fig. 1). According to tectonics shape feature and fault distribution, Daning-Jixian Block is divided into four structural domains, i.e., the eastern slope zone (B1), Puxian depression zone (B2), Guyi-Yaoqu anticline and fault zone (B3) and western slope belt (B4).

Block B1 locates in the south-east of study area. Morphologically, block B1 is a northwest-dipping monocline with an inclination angle of 3°–6°. Block B2 is a depression, formed by extrusion, which locates in the northeast of study area. Some small normal faults are developed in this domain. Block B3 is a northeast–southwest structural belt, which locates in the middle of study area. The Xueguan-Yukou thrust fault is distributed in this domain, which is accompanied by several small

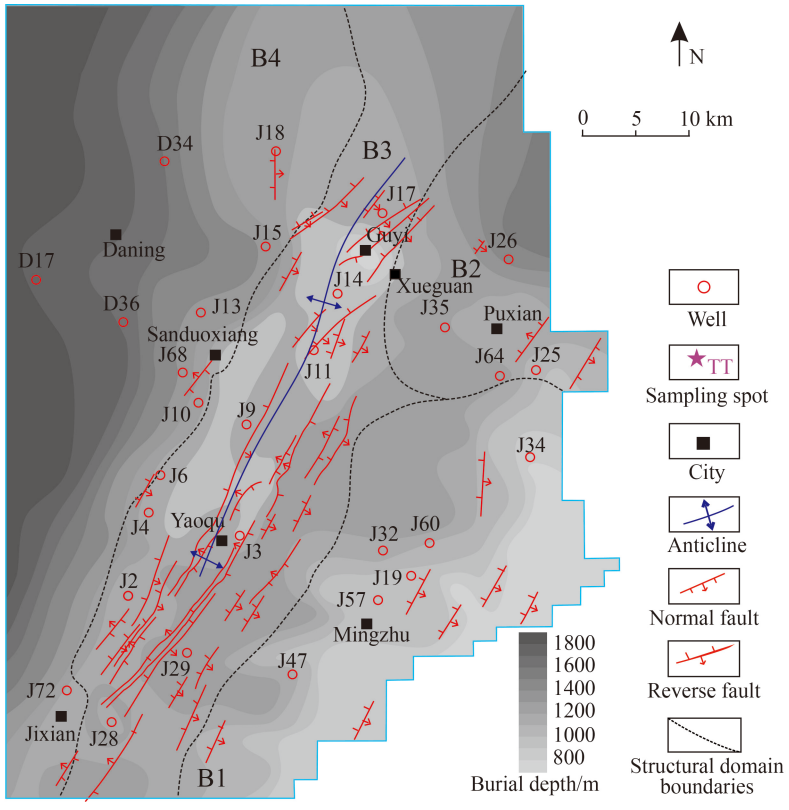

Fig. 1 Structural burial depth outline of the bottom of the No. 8 coal seam in Daning-Jixian CBM Block. B1–B4 are structural domains.

thrust faults. Affected by the traction of the Xueguan-Yukou reverse fault, a long-axis anticline was formed in this domain with structural amplitude of 80–120 m and an axis length of about 40 km. Block B4 is a gentle slope zone in the west of study area, with a dip angle of 0.3°–2.5°.

The strata preserved in Daning-Jixian Block include rocks of the Archaeozoic, Proterozoic, Cambrian, Ordovician, Carboniferous, Permian, Triassic, and Quaternary Systems (Fig. 2). Multi coal seams (No.1–8) are developed in Carboniferous-Permian coal-bearing strata (Fig. 2). The fluvial-deltaic environmental No. 5 coal of Shanxi Formation and shallow-marine environmental No. 8 coal of Taiyuan Formation are the main target coal seams for CBM production in this area, with thickness of 0.5–8 m and 3–9.8 m, respectively. The vitrinite reflectance ($R_{o,\,max}$, %) of organic matter in these two coal seams is about 1.37%–3.40%, belonging to the coal rank of middle-volatile bituminous, semi-anthracite and anthracite.

3 Method and data set

3.1 Sample and experiments

Two coal samples were collected from fresh coal mining face in underground coal mines which adjoin our study area (Fig. 1). To minimize the influence of tectonic deformation and macroscopic coal type on the experimental results, primary structural and semi-bright coals were selected for experiments. Samples were crushed and sieved to a size range of 0.18–0.25 mm (i.e., 60–80 mesh),

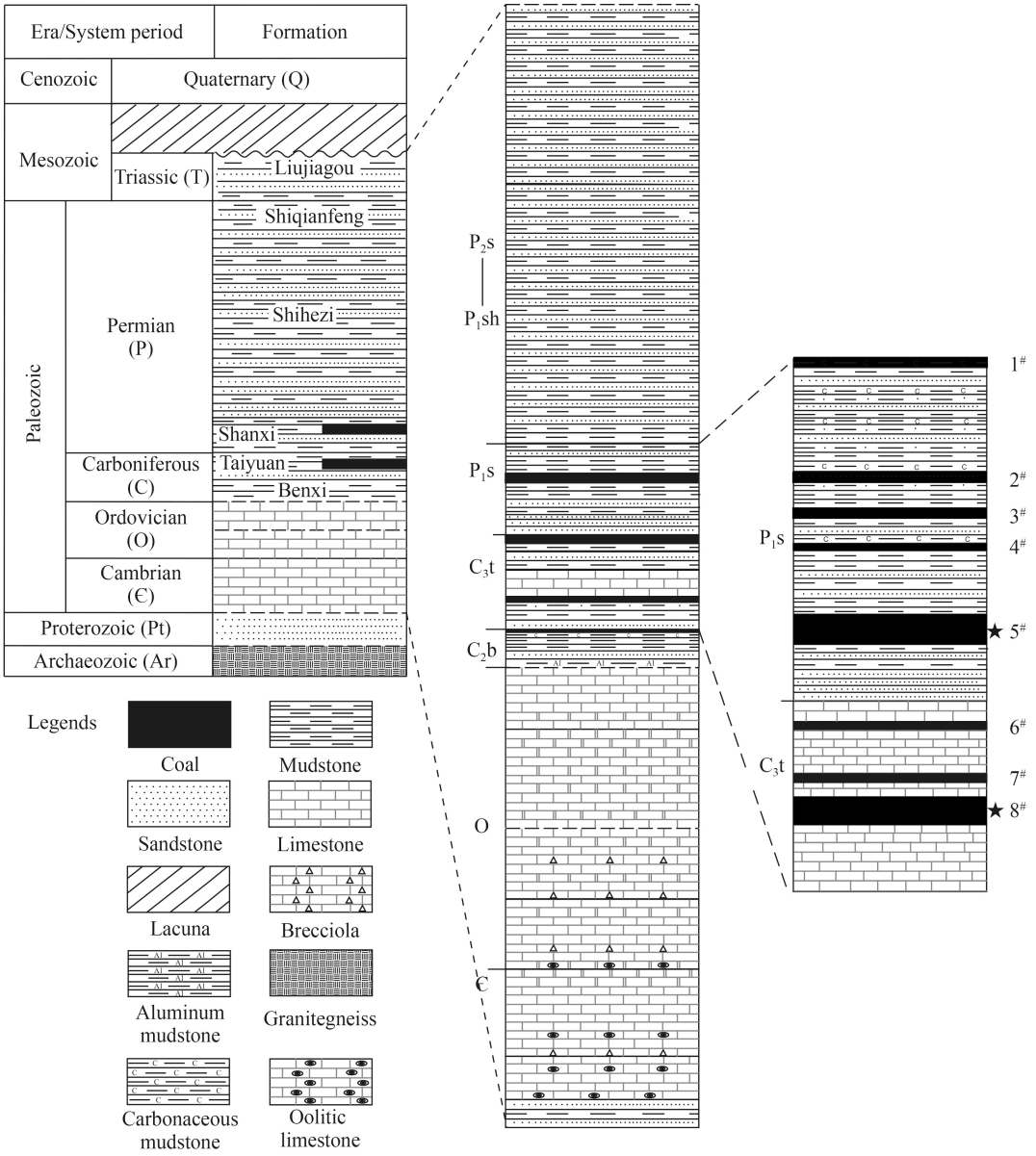

Fig. 2 Stratigraphic column of the Daning-Jixian CBM Block. The dashed lines indicate the formation unconformity.

and moisture-equilibrium treatment was completed. Then, a series of isothermal adsorption experiments were carried out at 35°C, 45°C, and 55°C under an equilibrium pressure of up to 20 MPa. Combining with the simulated results of coal reservoir conditions (pressure and temperature) evolution, these isotherms were used to characterize the adsorption capacity evolution character of coal reservoir during uplift process.

3.2 Simulation process

Data of 13 exploration wells were used to simulate the evolution of coal reservoir. The fundamental data that includes proximate analysis, coal seam burial depth, thickness, vitrinite reflectance, gas content and others were used for numerical simulation. Table 1 provides an example of the input database of the Well J2.

The dynamic equilibrium model used in our previous work (Yan et al., 2015, 2021b) which proposed by Wei et al. (2007, 2010), was also used in this study for the simulation of reservoir geological evolution history. The tectonic subsidence history, geothermal field evolution history and methane generation features were simulated by using a commercial computer software program PetroMod 2016. More details can be found in our previous work (Yan et al., 2015, 2021b).

4 Result and discussion

4.1 Tectonic and subsidence evolution

In the Archaean and Proterozoic Era, as a part of the North China Platform, the Ordos Basin was in a relatively stable stage. In the Early Paleozoic Cambrian and Ordovician periods, the study area was in neritic sedimentary environment (Philip et al., 2009), a large number of marine strata were deposited in this period. Then, the study area experienced a long-term depositional gap from the Early Paleozoic to Late Paleozoic, resulting in the lack of Late Ordovician, Silurian, Devonian and Early Carboniferous strata. After that, coal-bearing strata were deposited in the period of the Middle and Late Carboniferous–Early Permian. These coal-bearing strata that enriched organic went through a series of burial and uplift processes (Figs. 3 and 4), which can be divided into six stages.

4.1.1 Stage I: Middle-Late Carboniferous and Permian Periods

The study area changed from uplifting to subsidence stage due to Hercynian crustal orogeny. The fluvial-deltaic environmental Shanxi Formation and shallow-marine environmental Taiyuan Formation coal-bearing strata were deposited in this period (Fig. 4(a)). The deposition speed was 3.3–12.1 m/Ma and 4.4–13.9 m/Ma, respectively. The sedimentary thickness was 25–91 m and 63.9–202.5 m, respectively (Figs. 5(a) and 5(b)). In the Carboniferous Period, the sedimentary center was located near wells J25, J34, and J13 in eastern study area. The deposition speed increased from west to east, and, the coal-bearing strata thickness of Taiyuan Formation gradually increased from west to east. Then, the sedimentary center shifted southward, in the region near Well J47, with a sedimentary thickness of more than 200 m. The deposition thickness was thinner in central study area, ranging from 60 m to 80 m (Fig. 5(b)). At the end of Early Permian Period, the total thickness of coal-bearing strata gradually thickened from north-west to south-east, and the maximum thickness reached about 250 m near Well J47 in the south-east (Fig. 5(c)). Then, the subsidence

Table 1 Database of simulation nodes that contain Well J2

Parameter	Value	Parameter	Value
X [a)]	19475810	Y [a)]	4007477
Recent burial depth [a)]/m	1135.8	V_L [a)]/($m^3 \cdot t^{-1}$)	24.49
P_L [a)]/MPa	1.92	Reservoir pressure [a)]/MPa	8.56
Gas content in air dry basis [a)]/($m^3 \cdot t^{-1}$)	14.4	Gas saturation [a)]/%	64.57
Moisture [a)]/%	0.78	Ash yield [a)]/%	16.78
Vitrinite [a)]/%	73.1	Inertinite [a)]/%	13.6
Liptinite [a)]/%	–	Volatile matter [a)]/%	10.48
Coal thickness [a)]/m	4.6	$R_{o,max}$ [a)]/%	2.29
Turning point of R_o [b)] /Ma	299, 251, 203.6, 189.6, 175.6, 145.5, 130	$R_{o,max}$ at turning point [b)]/%	0.28, 0.45, 0.76, 0.79, 0.82, 1, 2.29
Burial depth turning point of bottom coal seam[b)]/Ma	299, 251, 203.6, 189.6, 175.6, 145.5, 130, 65.5, 1.806, 0	Burial depth of bottom coal seam at turning point [b)]/ m	46.5, 790.1, 2799.5, 2404.1, 2634.1, 2324.1, 3134.1, 1784.1, 1114.1, 1135.8
Turing point of geo-temperature gradient[b)]/Ma	306.5, 235, 160, 153, 130, 124, 100, 50,0	Geo-temperature gradient at turning point [b)]/(°C·10^{-2} m^{-1})	2.8, 3, 3.2, 3.2, 7.17, 3.2, 3.2, 3.05, 2.9

Notes: V_L and P_L are Langmuir volume (in air-dry base) and Langmuir pressure. [a)] The data are obtained from wellbore and geophysical logging. [b)] The data are obtained from the deposition burial, geothermal, and organic maturation history simulations.

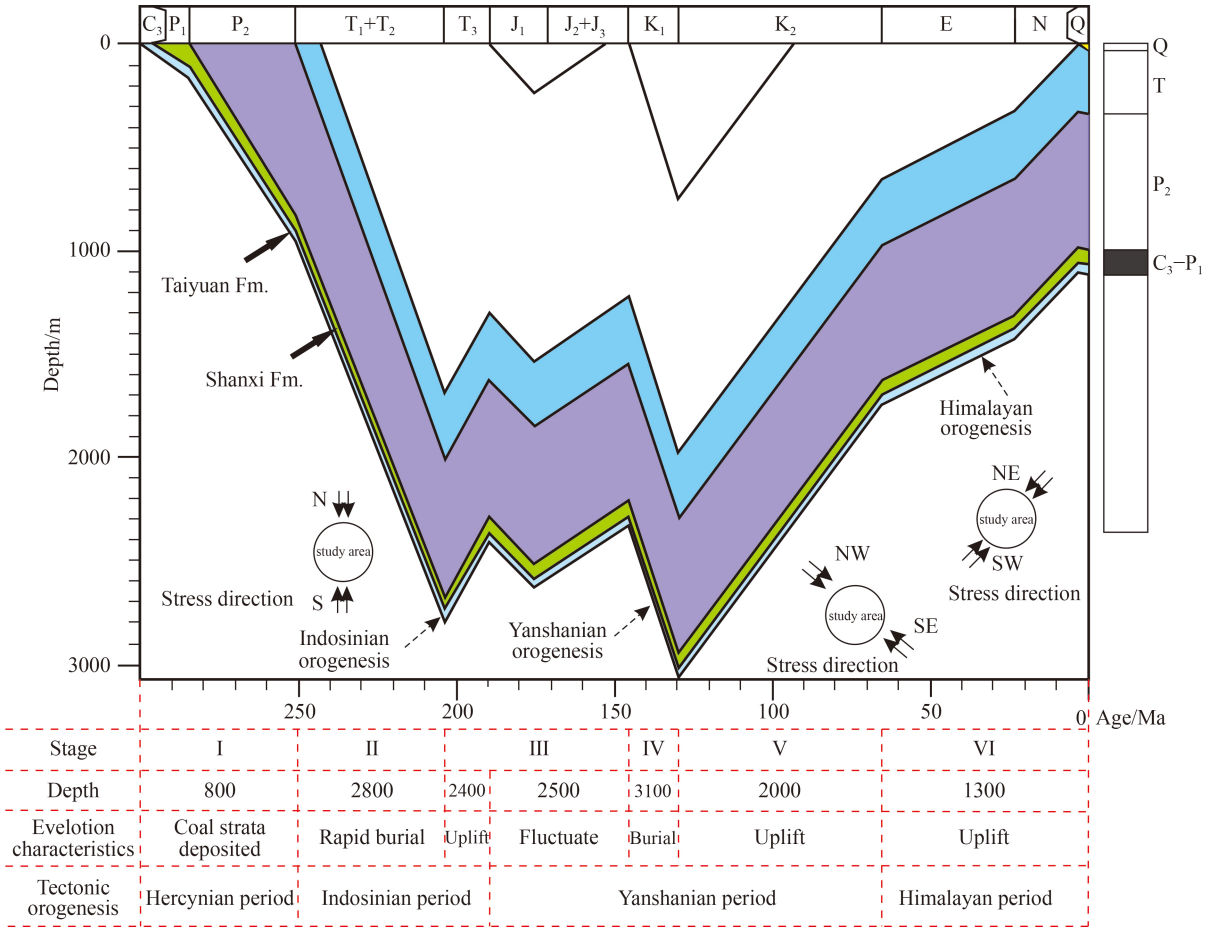

Fig. 3 Typical tectonic movement and burial history curve for the coal-bearing strata in the study area.

speed increased to approximately 17.61–31.86 m/Ma in the Late Permian Period, and the sedimentary thickness was 588–1064 m in the Shihezi and Shiqianfeng Periods (Fig. 6(a)). During this stage, the sedimentary center was located near Puxian, and the sedimentary thickness reached more than 1000 m. At the end of this evolution period, the burial depth of coal-bearing strata generally increased from south-west to north-east, and reached the maximum burial depth of about 1200 m in Puxian area (Fig. 6(b)).

4.1.2 Stage II: Early and Middle Triassic Periods

Abundant river-lake face red clastic rocks i.e., Liujiagou Formation, Heshanggou Formation, Zhifang Formation and Yanchang Formation were deposited successively during the Early and Middle Triassic periods. The deposition speed was about 37.1–45.6 m/Ma, and the deposition thickness ranged from 1760 m to 2160 m. Thicker strata were deposited in the areas where thinner strata deposited in the previous evolution stage (Fig. 6(b), Fig. 7(a)). At the end of this stage, the burial depth of the Taiyuan Formation increased gradually from south-east to north-west in study area (Fig. 4(b); Fig. 7(b)). In Puxian region, where the previous sedimentary strata were relatively thicker, the buried depth reached more than 3000 m (Figs. 4(b) and 7(b)).

4.1.3 Stage III: Late Triassic Period to Late Jurassic Period

In the Late Triassic Period, a south-north compressive stress field was formed by the collision between the North China Plate and the Yangtze Plate during the Indosinian Orogeny (Fig. 4(c)). Affected by this compressive stress, the study area was uplifted and eroded with eroding speed was about 26.4–32.9 m/Ma. The eroding thickness was about 370–460 m (Fig. 8(a)). The Yanchang Formation was eroded in this period (Fig. 4(c)). At the end of Late Triassic, the buried depth of coal reservoir is about 2260–2660 m (Fig. 8(b)). In the following Early Jurassic Period, the study area experienced short-term deposition (Fig. 4(d)). Then, in the Middle and Late Jurassic Periods, a northwest–southeast compressive stress field was formed by the collision between the Paleo-Pacific Plate and the Eurasian Plate during the Early Yanshanian Orogeny (Fig. 3). Affected by this compressive stress, the study area was uplifted and eroded again (Fig. 4(e)), with eroding speed and the eroding thickness was about 7.6–12 m/Ma and 230–360 m, respectively (Fig. 9(a)). The anticlinal structural belt and the fracture system were

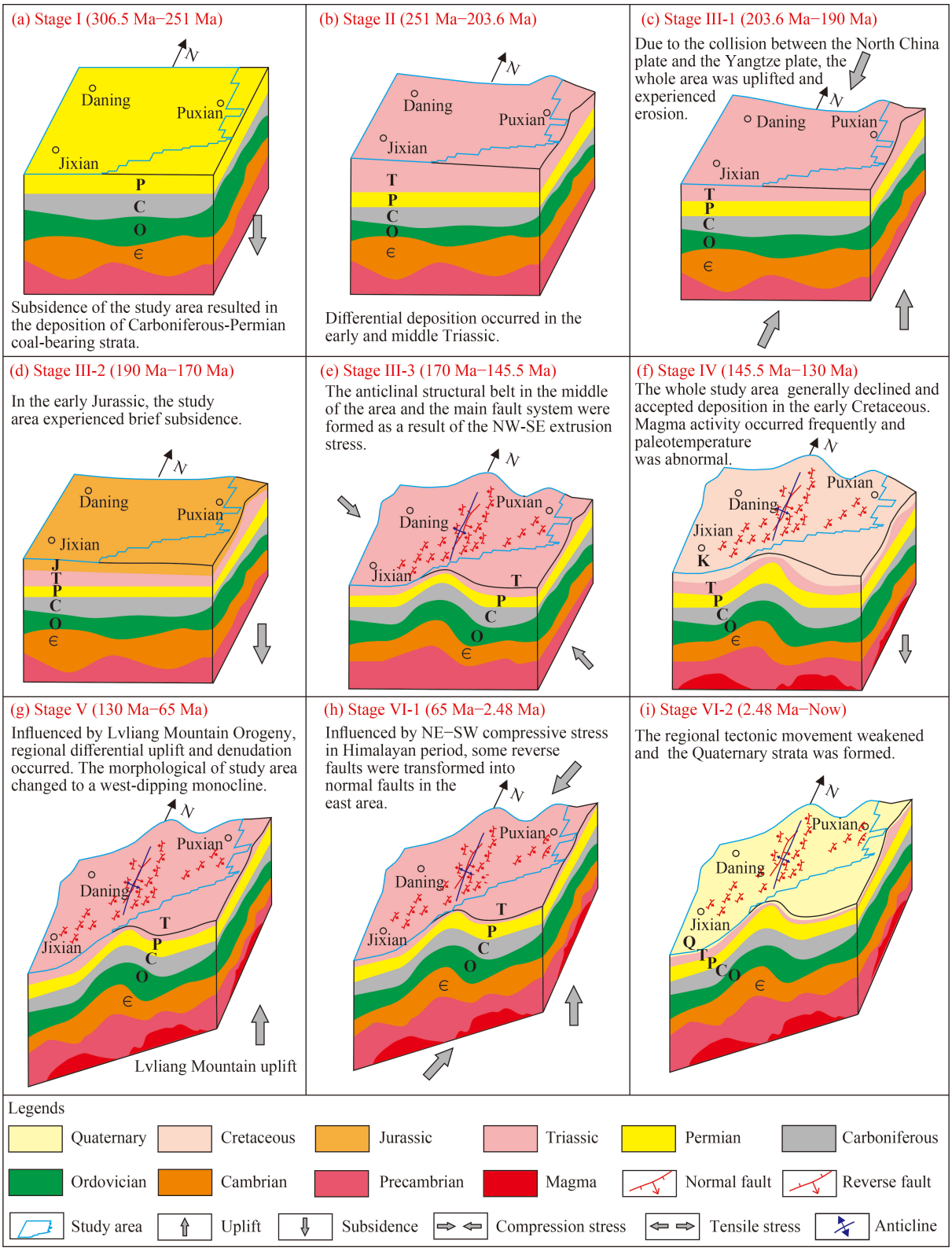

Fig. 4 Schematic diagram of the study area tectonic evolution.

also formed under this compressive stress in central region of study area (Fig. 4(e)) (Yang et al., 2013). The tectonic pattern of the study area was basically formed in this evolution stage (Fig. 9(b)).

4.1.4 Stage IV: the Early Cretaceous Period

During the fourth stage, subsidence occurred throughout the study area as a result of the Middle Yanshanian

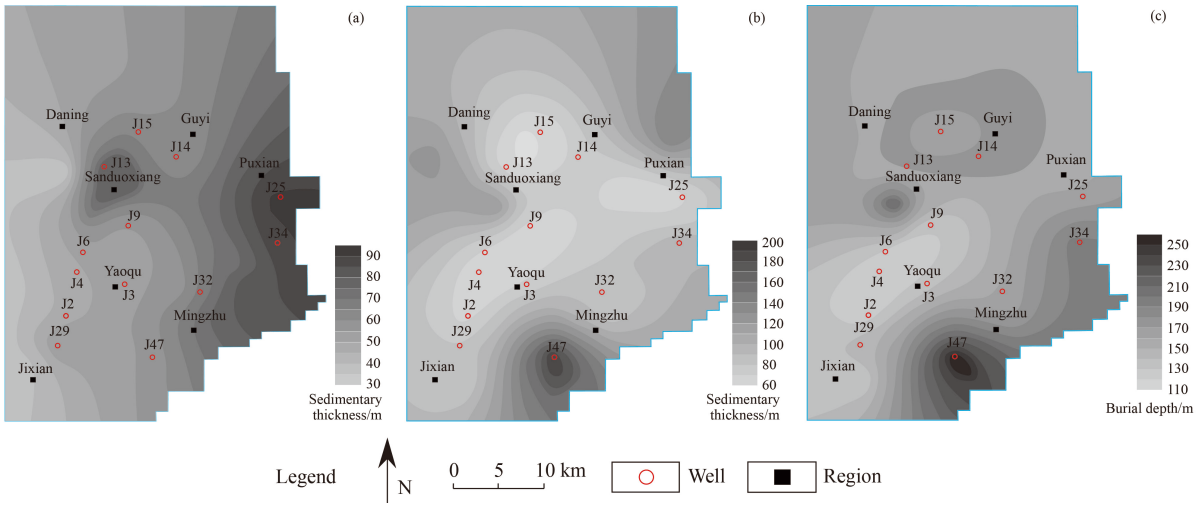

Fig. 5 Sedimentary characteristic distribution of coal-bearing rock series: sedimentary thickness of Carboniferous Taiyuan Formation (a); sedimentary thickness of Permian Shanxi Formation (b); burial depth of the bottom in Taiyuan Formation at the end of the Permian Shanxi period (c).

Orogeny (Fig. 4(f)). The deposition thickness reached about 700–1100 m in Puxian region (Niu et al., 2010). The Permo-Carboniferous coal-bearing strata were deep buried again. The burial depth reached the maximum value about more than 3000 m. Increasing magma-heat events occurred as a result of the Middle Yanshanian Orogeny (Fig. 4(f)) (Cao et al., 2018; Li et al., 2022).

4.1.5 Stage V: the Late Cretaceous period

In this stage, the study area was uplifted and eroded again due to the uplift of the Lvliang Mountain Orogeny (Fig. 4(g)). The south-east part of study area uplifted most and the whole block was inclined to west in this stage (Wang et al., 2013). The eroding speed and the eroding thickness were about 14.3–23.6 m/Ma and 920–1520 um, respectively (Fig. 10(a)). At the end of this stage, the burial depth of the Taiyuan Formation increased gradually from the central area to the surrounding area in study area (Fig. 4(g); Fig. 10(b)).

4.1.6 Stage VI: Cenozoic Era and Quaternary

During the Cenozoic Era, the regional stress field changed

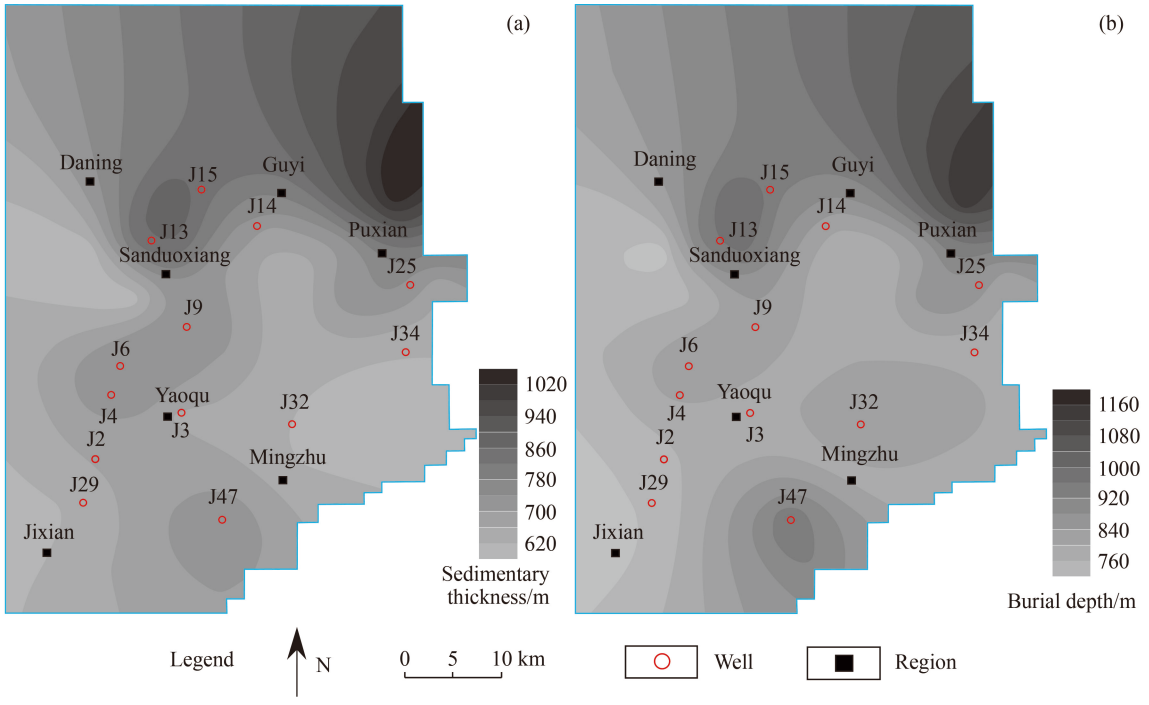

Fig. 6 Sedimentary thickness distribution in the Shihezi and Shiqianfeng periods (a), burial depth of the bottom in Taiyuan Formation at the end of the Permian stage (b).

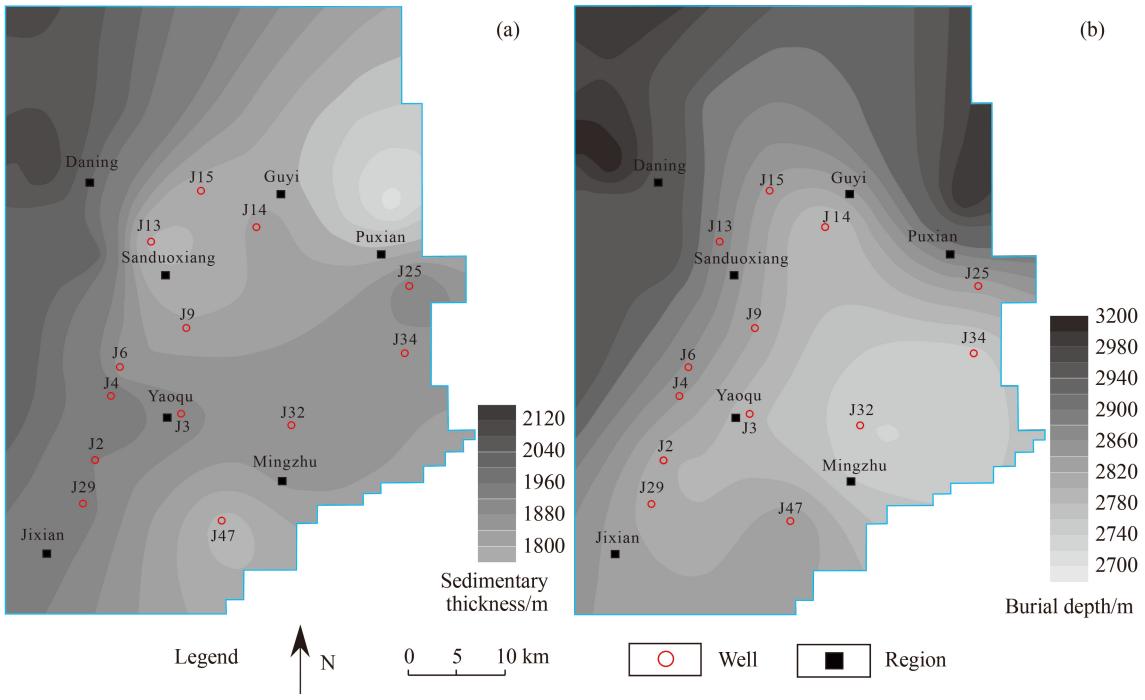

Fig. 7 Sedimentary thickness distribution during the Early and Middle Triassic stage (a), burial depth of the bottom in Taiyuan Formation at the end of Middle Triassic stage (b).

to northeast–southwest direction. Affected by this variation of regional stress field, some reverse faults were transformed into normal faults in the Puxian area (Fig. 4(h)) (e.g., the region of Well J25) (Tian et al., 2012). The structural framework of the study area was basically formed (Figs. 11(a), 11(b)). During this period, the research area continued to be uplifted and eroded (Fig. 3). The erosion thickness was approximately 540–900 m, with a speed of 8.5–14.1 m/Ma (Fig. 11(a)). The sedimentary strata eroded most in the south-east region. During the last evolution period (i.e. Quaternary period), a set of mudstones was deposited in study area, with a deposition rate of 3–

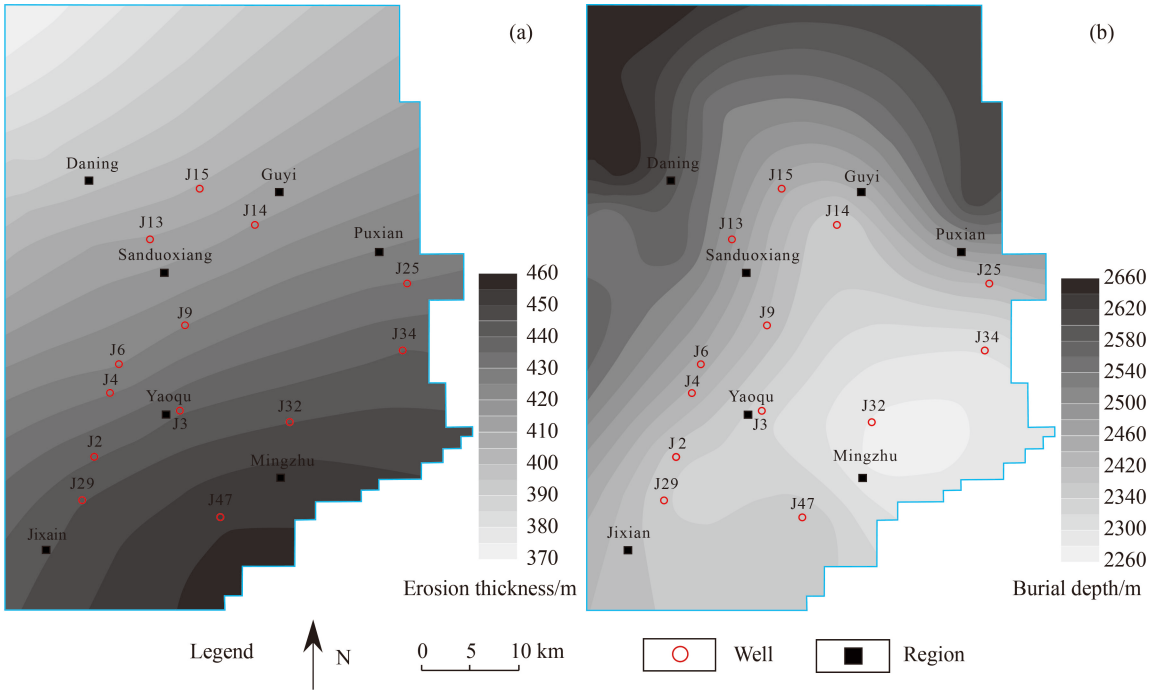

Fig. 8 Erosion thickness distribution during the Late Triassic Period (a), burial depth of the bottom in Taiyuan Formation at the end of the Triassic Period (b).

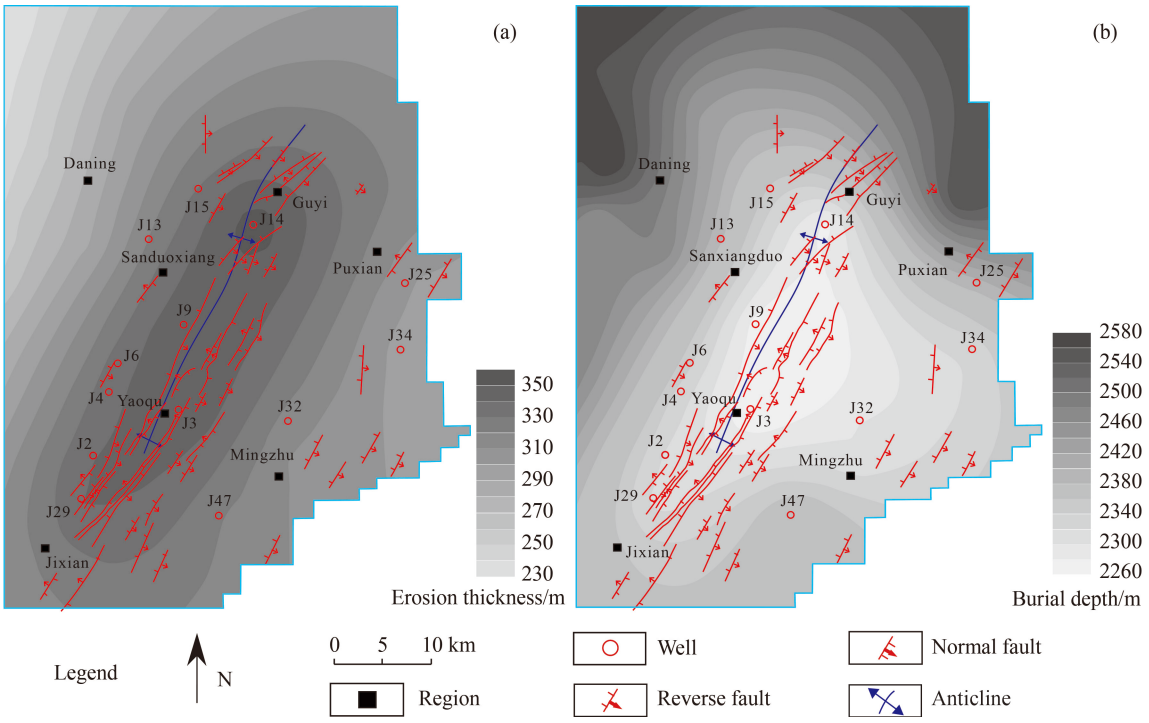

Fig. 9 Erosion thickness distribution during the Jurassic Period (a), burial depth of the bottom in Taiyuan Formation at the end of the Jurassic Period (b).

84 m/Ma and a deposition thickness of 0–170 m (Figs. 4(i) and 12(a)). The deposition thickness decreased from the middle to the surrounding area. Then, the burial depth characteristic of the Taiyuan Formation and tectonic pattern of the study area were formed (Fig. 12(b)).

4.2 Geothermal evolution and coal maturation

The thermal evolution history of the study area can be divided into six stages according to the subsidence and paleogeothermal gradient evolution history (Fig. 13).

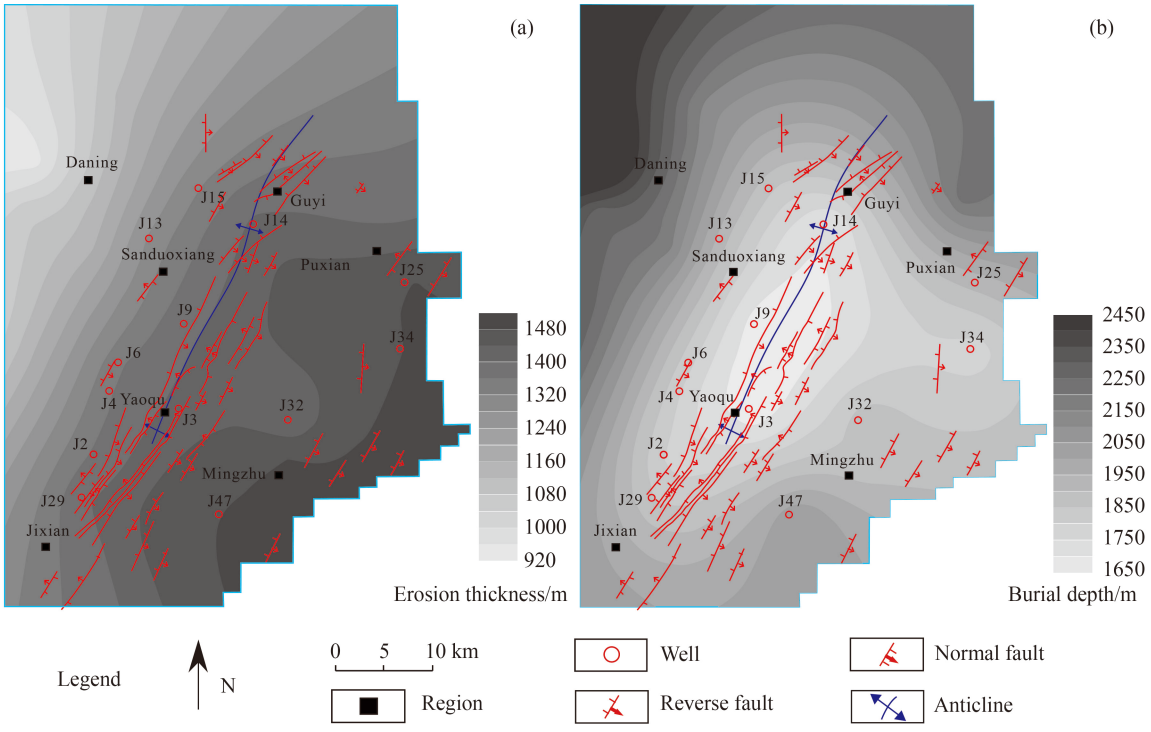

Fig. 10 Erosion thickness distribution during Late Cretaceous Period (a), burial depth of the bottom in Taiyuan Formation at the end of Late Cretaceous Period (b).

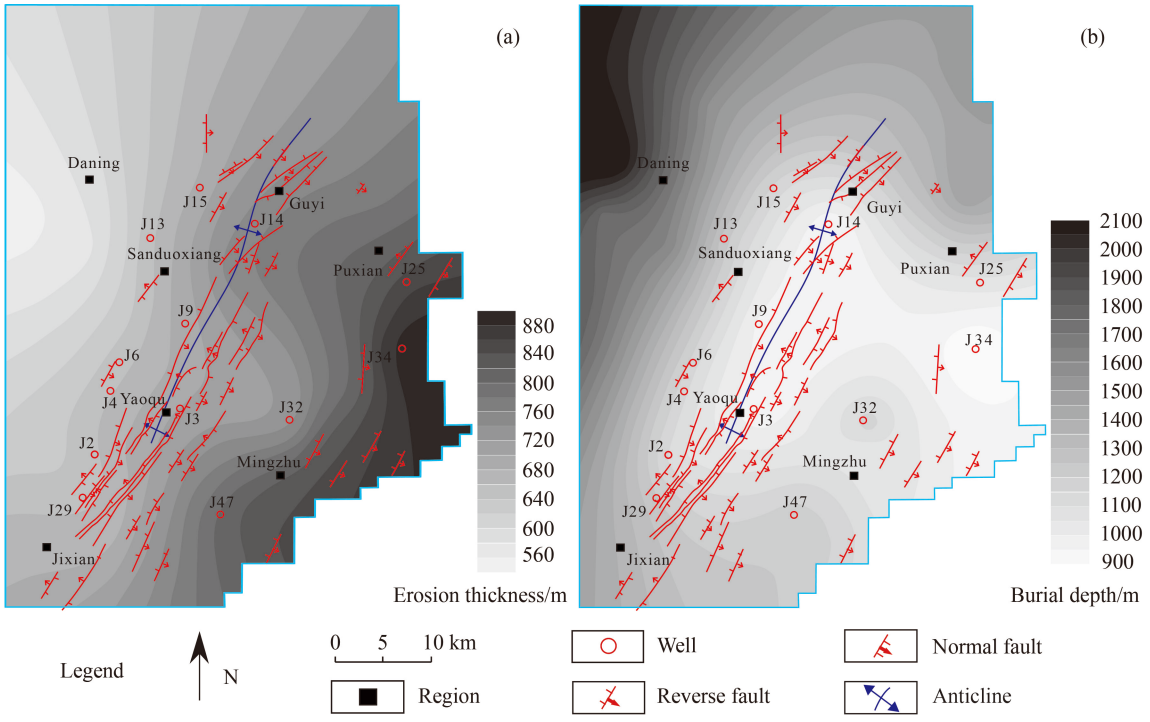

Fig. 11 Erosion thickness distribution during the Paleogene and Neogene Periods (a), burial depth of the bottom in Taiyuan Formation at the end of the Neogene Period (b).

During stage I (306.5–251 Ma), geothermal gradient was 2.8°C/100 m. The coal reservoir was buried shallowly, and the maturity of organic matter was relatively low (Fig. 13). In stage II (251–203.6 Ma), due to the rapid subsidence, the coal reservoir temperature rose up to 114°C–119.6°C at the end of the Middle Triassic (Fig. 14 (a)). Coal-forming organic matter had undergone long-time plutonic metamorphism. The vitrinite reflectance of coal organic matter reached about 0.73%–0.77% (Fig. 14 (b)). In stage III (203.6–145.5 Ma), the temperature of the

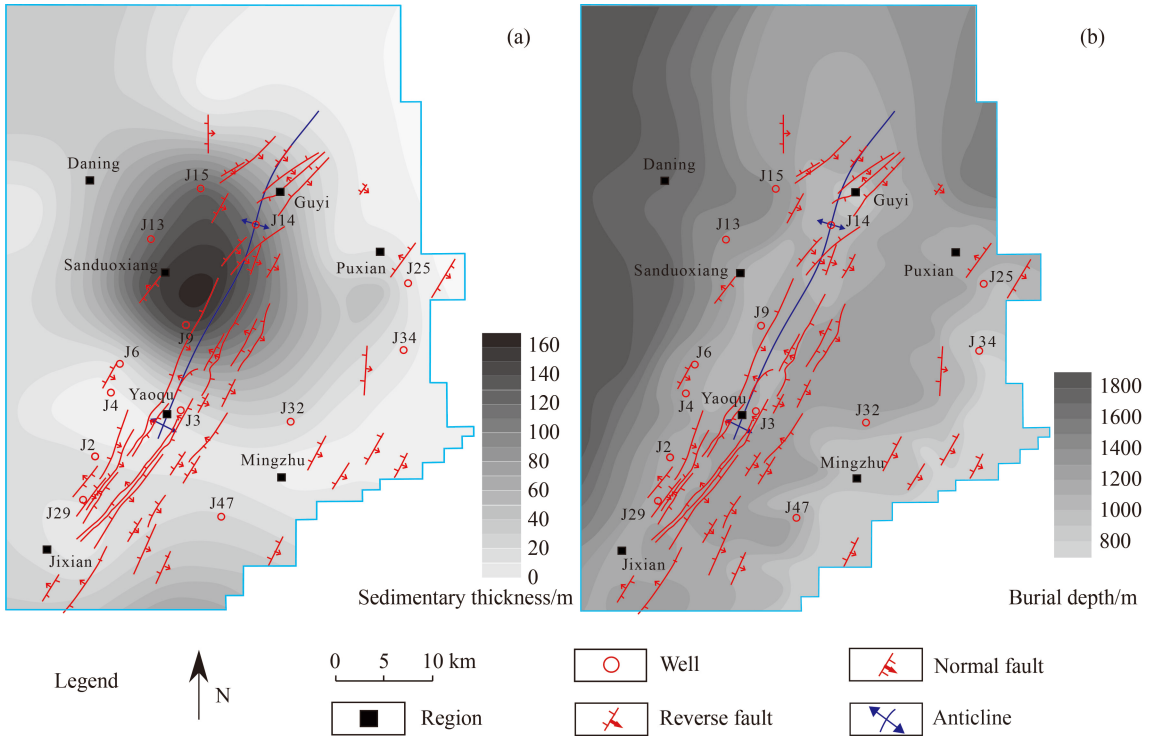

Fig. 12 Deposition thickness distribution during the Quaternary Period (a), current burial depth of the bottom in Taiyuan Formation (b).

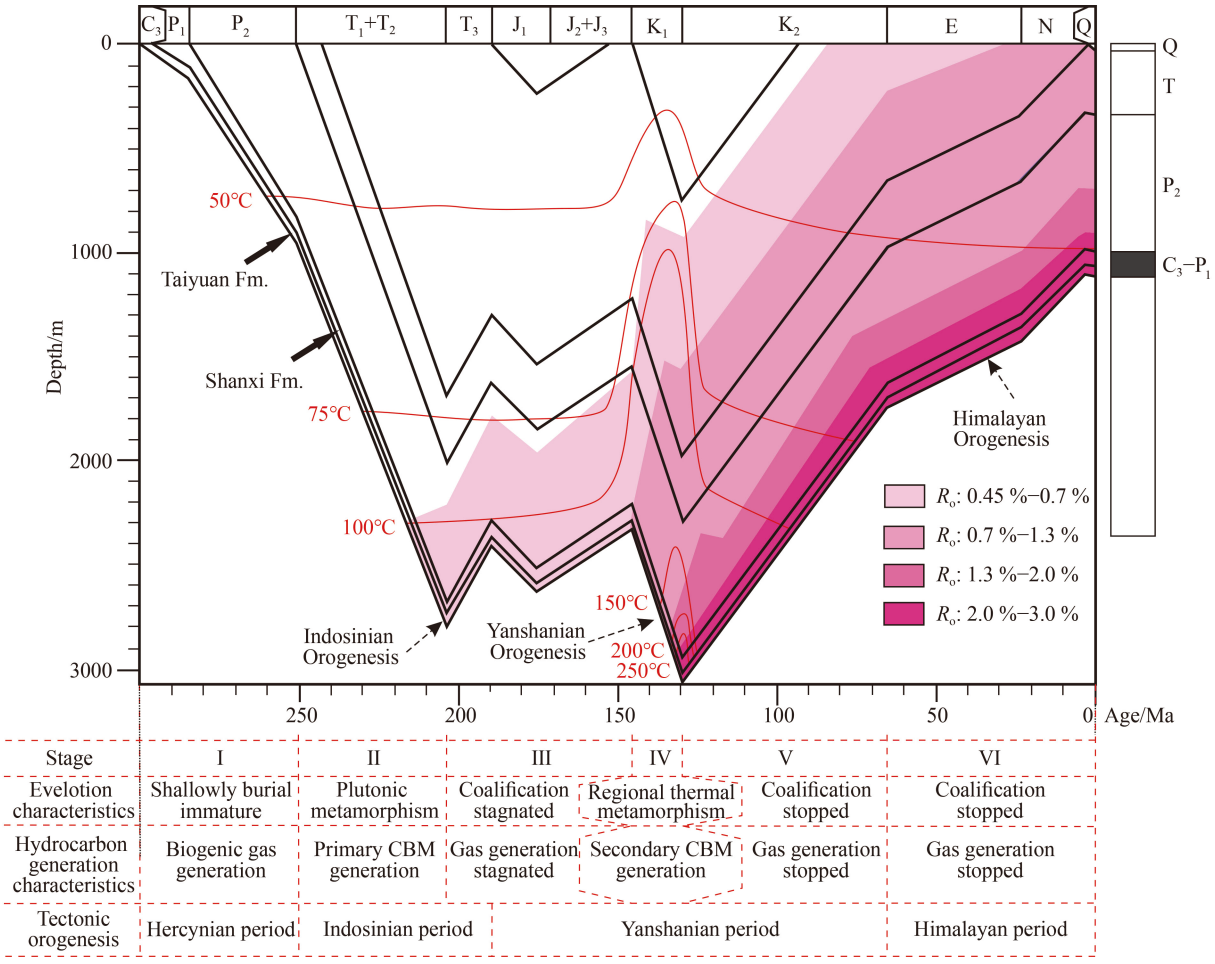

Fig. 13 Thermal evolution history in the study area.

coal reservoir decreased because of the tectonic movement occurring during the Late Triassic–Jurassic (Fig. 13). Then, during the stage IV (145.5–130 Ma), coal-bearing strata was buried deeply again. Affected by regional thermal metamorphism, the temperature of coal reservoir rapidly raised to about 210°C–310°C (Fig. 15 (a)). The maximum vitrinite reflectance of coal organic matter reached 1.60%–3.4% (Fig. 15(b)). Later the study area was uplifted rapidly and suffered denudation, and the geothermal gradient gradually returned to normal. For the last two stages, the geothermal field reverted to a lower level, and the geo-temperature substantially decreased (Fig. 13). Coal organic matter stopped maturing during those two stages.

4.3 CBM accumulation process

In each evolution stage, the *in situ* gas content of the coal seam was mainly affected by the synthetic effects of coal adsorption capacity and reservoir conditions (pressure and temperature). An experimental simulation method that modified from Bustin and Bustin (2008) was used to investigate the evolutionary process of CBM accumulation in our previous works (Yan et al., 2015, 2021b). In this work, a similar experimental simulation work was also conducted. The coal adsorption capacity increases whiles the pressure and temperature of coal reservoir decrease (i.e., the uplifting process) (Fig. 16). Table 2 shows the adsorption capacity evolution characteristics in the domains of B1 and B2 during the uplifting process in Cenozoic Era and Quaternary Period.

The experimental results shown in Fig. 16 and Table 2 were used to simulate the CBM accumulation processes and the formation history combining with the results from simulation using the dynamic equilibrium mode. The output of the simulation includes many evolution characteristics of reservoir parameters (i.e., burial depth; cumulative gas production; cumulative gas diffusion; R_o; *in situ* gas content at each geological time; and gas production, diffusion and retention features during each geological evolutionary stage). Table 3 provides an example of the simulation results for simulation nodes that contain Well J2. The evolution of the CBM reservoir of the No. 8 coal is shown in Fig. 17. The evolution history of CBM reservoir formation in the study area can also be divided into six stages in accordance with the subsidence (Fig. 3) and paleo-geothermal (Fig. 13) evolution history.

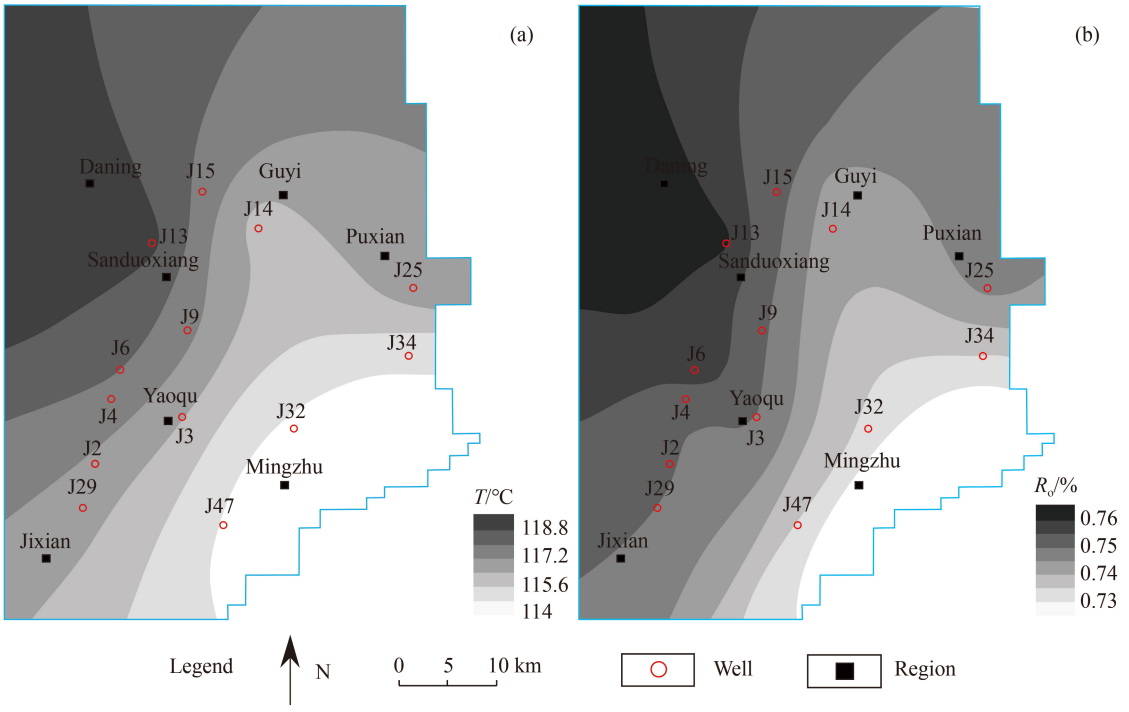

Fig. 14 Distribution characteristics of paleotemperature (a) and maturity (b) in the study area at the end of the Middle Triassic.

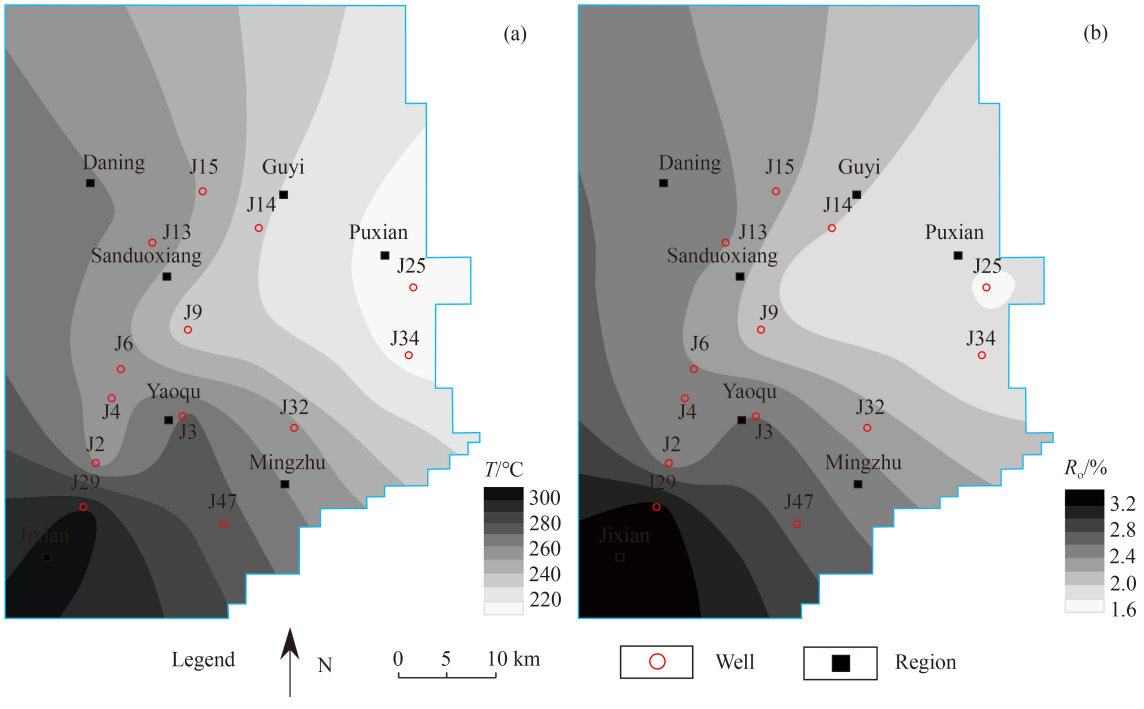

Fig. 15 Distribution characteristics of paleotemperature (a) and maturity (b) in the study area at the end of the Early Cretaceous.

The first stage is the main formation period of coal-bearing strata (306.5–251 Ma). In this period, the coal reservoirs were buried shallowly and the maturity of organic matter was low. Hydrocarbon generation was mainly consisted of biogenic gas which almost completely escaped due to the shallow depth and absence of an effective local reservoir cap. The second stage (251–203.6 Ma) is the rapidly burial stage. With the increasing of coal reservoir temperature, coal-forming organic matter suffered long-term plutonic metamorphism. The first significant hydrocarbon (i.e., primary plutonic metamorphism CBM) generation occurred in this stage. A few amounts of this primary CBM were stored in coal seam, while most was dissipated through diffusion. Subsequently, in the third stage (203.6–145.5 Ma), affected by the tectonic movement from the Late Triassic to

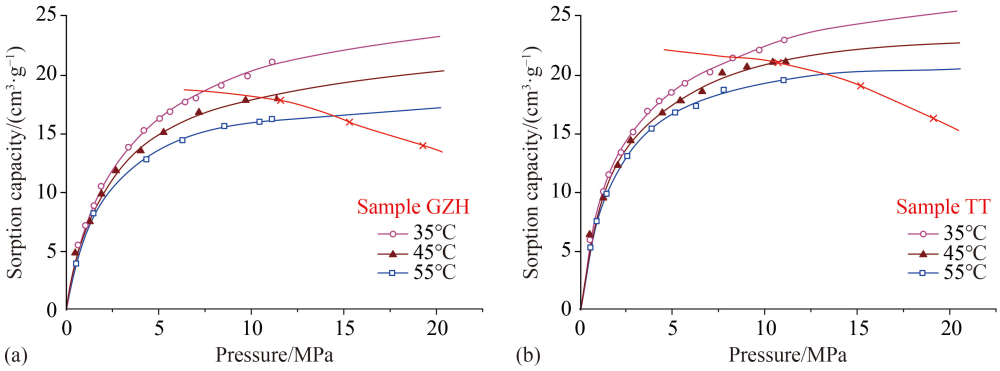

Fig. 16 The methane adsorption capacity at different temperatures and pressures. Two samples of GZH (a), TT (b) are from the domains of B2 (sample a) and B1 (sample b), respectively. The sorption capacities curve (red line) was plotted at the pressure and temperature conditions from reservoir subsidence and geothermal field history (the pressure gradient was set as 1.0 MPa/100 m).

Table 2 The sorption capacity, gas content and saturation evolution characteristics of the sampling sites during the uplifting process in Cenozoic Era and Quaternary Period

Structural domain	Sample	Parameter	Age/Ma		
			0	23.3	65.5
B1	TT	Depth/m	1164.7	1538	1942
		Q_S/(cm³·g⁻¹)	11.28	14.05	16.16
		P/MPa	11.65	15.38	19.42
		Q_C/(cm³·g⁻¹)	21.13	19.00	15.96
		S/%	53.38	73.91	100.01
B2	GZH	Depth/m	1076.8	1510	1921
		Q_S/(cm³·g⁻¹)	6.1	16.82	21.26
		P/MPa	10.77	15.1	19.21
		Q_C/(cm³·g⁻¹)	17.62	16.02	14.07
		S/%	34.62	105.00	151.13

Notes: Q_S and P are the gas content and reservoir pressure which were obtained from the simulations of CBM reservoir accumulation history. Q_C is the sorption capacity obtained from the adsorption capacity evolution simulation. S is the gas saturation of the sampling sites.

Jurassic, the coal-bearing strata are in an uplifting and fluctuant condition. The coal reservoir temperature decreased a lot, and the coalification was stagnant while hydrocarbon generation stopped. In the fourth stage (145.5–130 Ma), the coal seam temperature rose rapidly affected by regional thermal metamorphism effect (Figs. 13 and 15(a)). Coal-forming organic matter rapidly matured, and huge amount of secondary thermogenic gas generated accompanied with strong gas diffusion. During stage V (130−65.5 Ma), geothermal gradient gradually returned to normal, the maturation of organic matter and generation of hydrocarbon ceased. During the last stage VI (65.5 Ma–now), a large amount of gas was diffused due to further eroded of the overlying strata, which was controlled by the Himalayan tectonic movement.

4.4 Hydrocarbon system evolution and geological control effects

There is one hydrocarbon system in Daning-Jixian area (Fig. 18). During the dynamic evolution histories of hydrocarbon accumulation (i.e., generation, expulsion, and migration processes), the organic matter experienced twice hydrocarbon generation and accumulation processes, which happened in the Early-Middle Indosinian and Middle Yanshanian (Fig. 18). The source rocks and reservoirs are Carboniferous Taiyuan Formation and Permian Shanxi Formation, while the late Permian strata works as seal rocks providing a suitable condition for gas preservation. The Hercynian movement, Indosinian movement, Yanshanian movement and Himalayan movement sequential affect the evolution process of coal-bearing strata. As showed in Fig. 18, the CBM accumulation process (e.g., gas generation, accumulation and

Table 3 The simulation results of simulation node which contains well J2

Stage	Geological Time/Ma	R_o/%	Reservoir temperature/°C	Cumulative gas production/(m³·t⁻¹)	Gas production in each stage/(m³·t⁻¹)	Gas diffusion in each stage/(m³·t⁻¹)	Cumulative gas Diffusion/(m³·t⁻¹)	Gas content/(m³·t⁻¹)
I	306.6–251	0.45	53.70	3.12	3.12	2.18	2.18	0.94
II	251–203.6	0.76	116.96	21.04	17.92	12.54	14.72	6.32
III	203.6–145.5	1	104.55	21.04	0	6	20.72	0.32
IV	145.5–130	2.29	254.93	177.14	156.1	130.54	151.26	25.88
V	130–65.5	2.29	74.48	177.14	0	8.61	159.87	17.27
VI	65.5–0	2.29	54.15	177.14	0	2.87	162.74	14.4

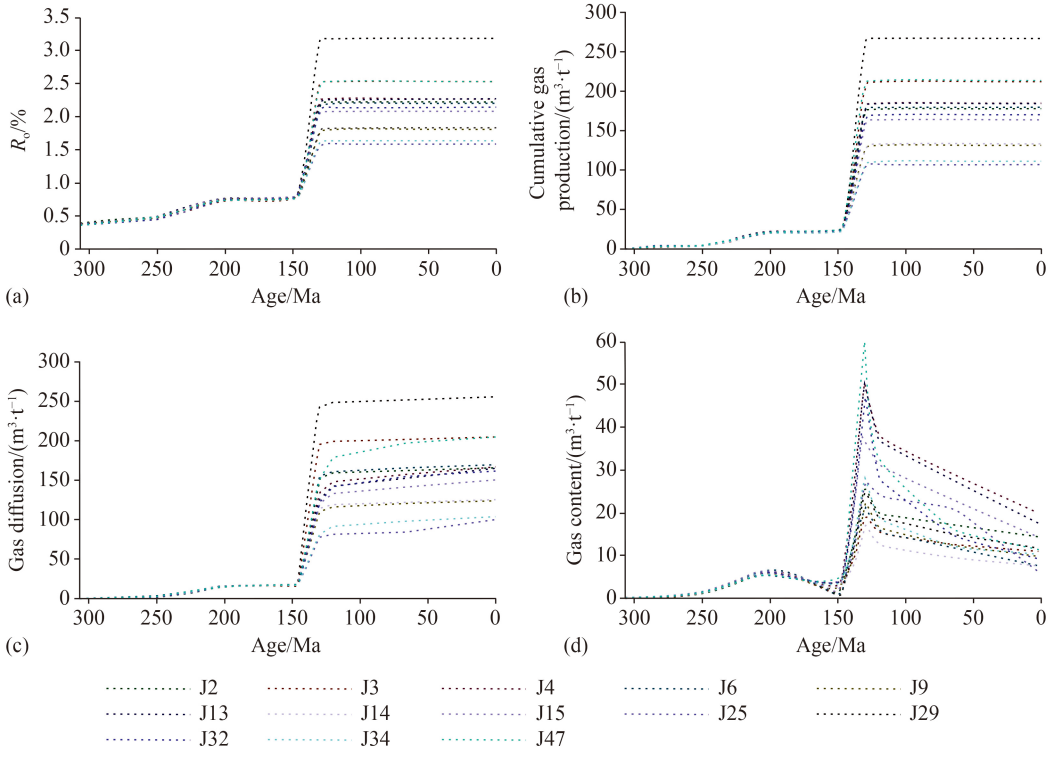

Fig. 17 Curves show the CBM reservoir formation evolution history: (a) cumulative gas generation; (b) coal organic maturity; (c) cumulative gas diffusion; (d) gas content.

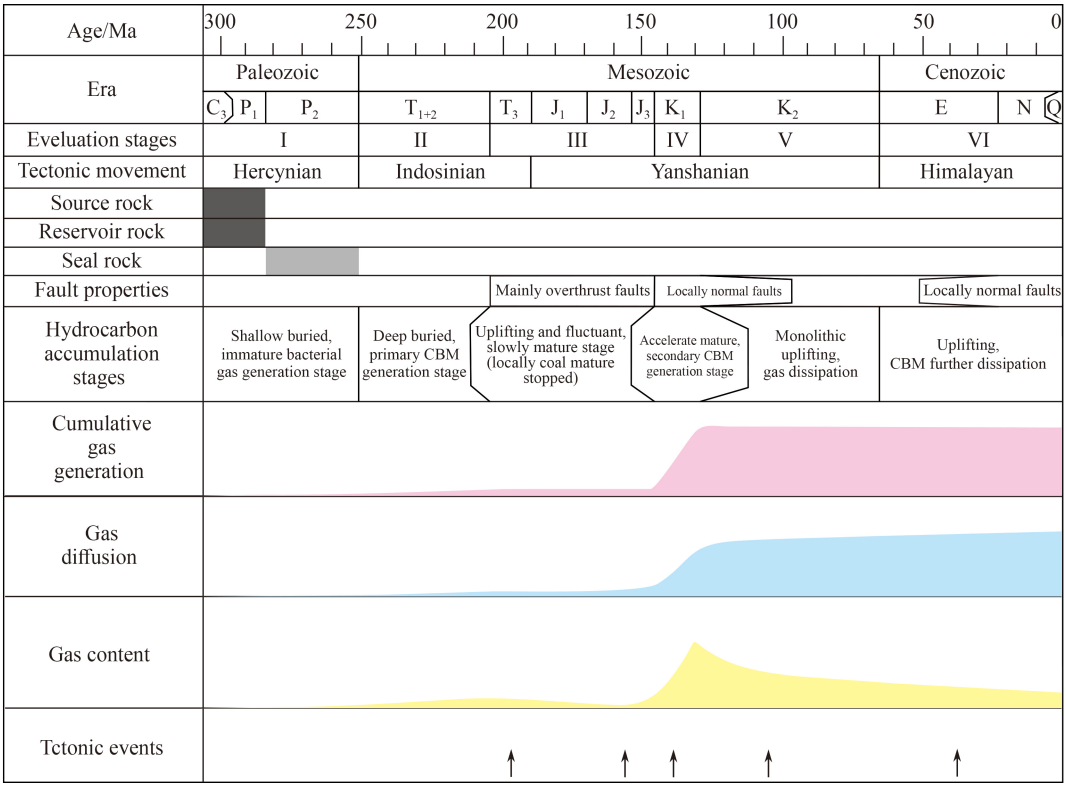

Fig. 18 Extended essential elements diagram showing the hydrocarbon system present in the study area with relation to tectonic activity and general fault behavior.

expulsion processes) was controlled by five tectonic events in study area, which led to the differential distribution of gas-bearing property at present.

During stage I, the generated gas is mainly composed of biogenic gas (306.5–251 Ma). The amount of gas generated was minimal and almost diffused due to poor storage and preserve conditions.

During stage II (251−203.6 Ma), the organic matter experienced primary thermogenic gas generation and accumulation processes. At this stage, the coal-bearing strata generated gas stably in the whole region and the huge thick strata which covered the coal reservoir provided a good capping condition. The accumulated dissipation and preserved gas content were in range of 13.8–15.8 m^3/t and 5.8–6.6 m^3/t, respectively (Figs. 19(a) and 19(b)). The regional distribution characteristic of accumulated dissipation and gas content was basically consistent with the distribution characteristic of coal reservoir maturity (Fig. 14(b)), which indicated a controlling mechanism of gas generation to gas dissipation and preservation.

The third stage is a CBM escaping stage (203.6–145.5 Ma). Influenced by the Late Triassic Indosinian movement (the first tectonic event) the study area was uplifted and denudated, which caused the paleo-geothermal temperature decreased and hydrocarbon generation stopped. Affected by this uplifting mechanism, the gas that generated in the early stage further diffused. During this stage, the amount of gas diffusion was about 0.5–1.5 m^3/t (Fig. 20(a)). By the end of the Triassic period, the gas content distribution characteristic was basically inherited from the previous period, and the gas content was about 4.5–6.1 m^3/t (Fig. 20(b)).

In the Early Jurassic, the study area experienced short-term deposition (in the early stage III). The hydrocarbon generation process was still stagnant as a response of relatively low paleo-geothermal. Then, during the Middle and Late Jurassic periods, affected by the Early Yanshanian movement (the second tectonic event), the study area was uplifted and eroded as a result of strong NW-SE compressive stress field. During this stage, the primary CBM generated in the stage II was further diffused. The total escaping amount was 3.0–6.2 m^3/t (Fig. 21(a)). Controlled by the compressive stress field, a regional anticlinal structural belt and a series of faults were formed in the middle of the region. The gas diffusion intensity in block B3 was stronger than other regions influenced by the development of these tectonic structures (e.g. the region of well J3). At the end of Jurassic, the gas content in the study area was 0–2.6 m^3/t, showing a trend of increasing from central region to north-western and south-western (Fig. 21(b)). Generally, the tectonic activities resulted in the regional gas escape divergence in this evolution stage, which caused the lower gas content in the central anticline fault zone than the other areas.

After the gas diffusion period (Stage III), the third critical tectonic event occurred in the Middle Yanshanian Orogeny (stage IV: 145–130 Ma).

In this stage, the magma-heat event resulted in an abnormal geothermal field and accelerated the coal matura-

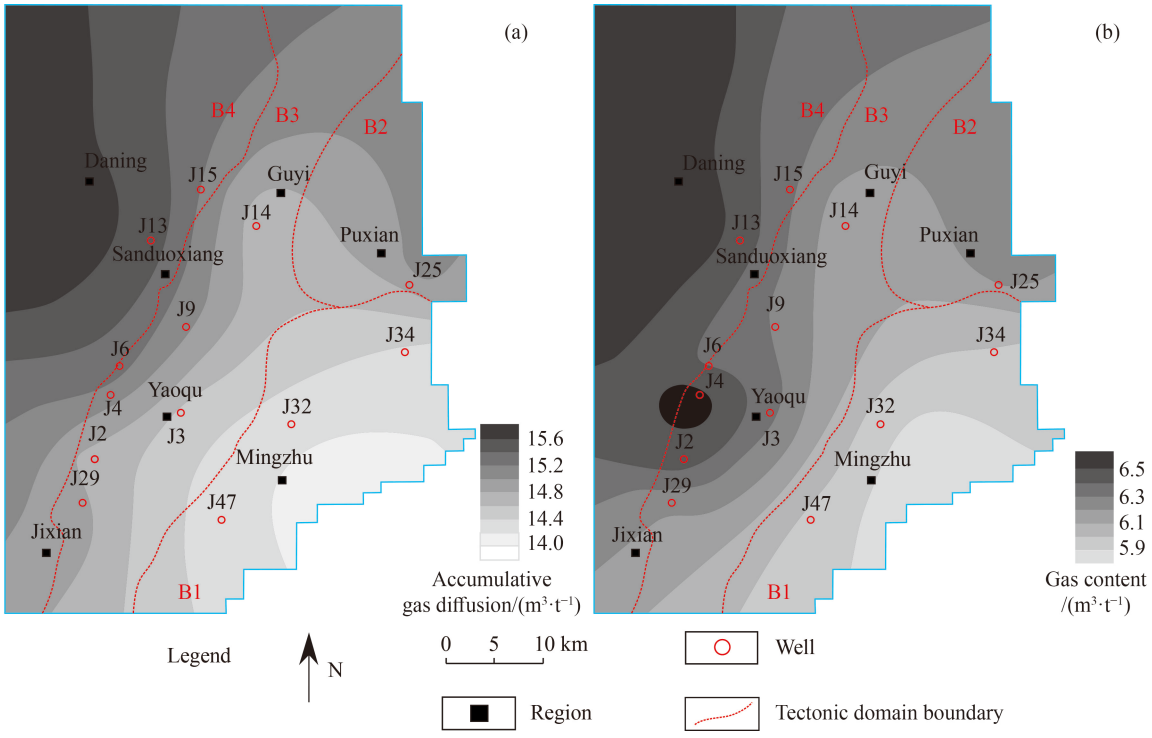

Fig. 19 Distribution characteristics of accumulative gas diffusion (a) and gas content (b) at the end of the Middle Triassic.

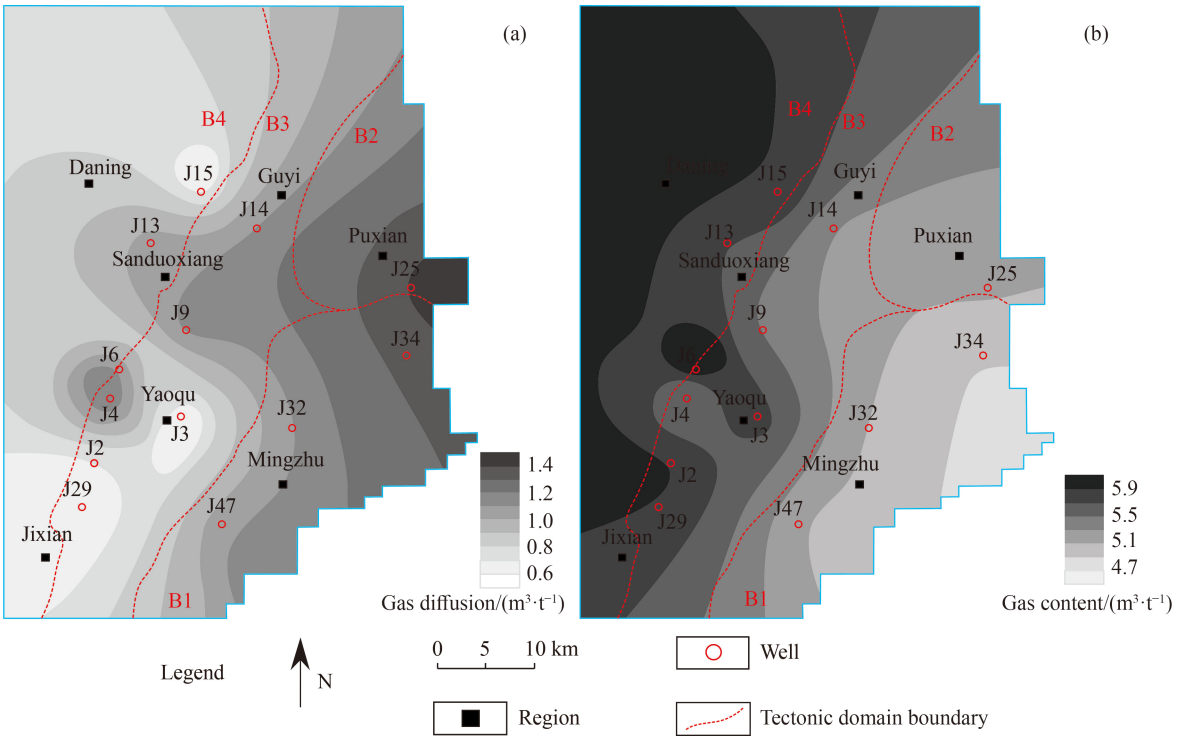

Fig. 20 Distribution characteristics of gas diffusion during the Late Triassic (a) and gas content at the end of the Late Triassic (b).

tion process. Hydrocarbon generation and diffusion reached their respective peak value over the entire geological evolutionary history. The heating center was in south-west of research area and radiated from south-west to north-east, and the vitrinite reflectance distribution and gas generation shown the same regularity. The total accumulated gas volume was about 106–265 m^3/t (Fig. 17). As the result of regional tensile stress field in this evolution period, the reverse faults that developed in the region of anticlinal-fault structural belt were transformed into normal faults (Wang et al., 2014). These opening faults system led to a large amount of gas escaped in this region. By the end of the Early Cretaceous, the accumulative amount of gas escaping was about 70–250 m^3/t (Fig. 22(a)). The final gas content of the study area was about 18–62 m^3/t by the end of this stage (Fig. 22(b)). The gas that preserved in the central anticlinal fault tectonic zone was less than other regions as a result of differential diffusion process.

During the stage V (130–65.5 Ma), the study area was uplifted by the Lvliang Mountains Orogeny (fourth tectonic event in the Late Yanshanian Orogeny), which resulted in the termination of coal thermal maturation and hydrocarbon generation (Stage V in Fig. 13). During this stage, the study area inclined to the west under the influence of south-east to north-west compressive stress. The uplifting amplitude gradually decreased from south-east to north-west. A large number of gases that preserved during the early evolution stages escaped, especially in the strong uplifting region. The total gas diffusion was about 6–46 m^3/t in this stage (Fig. 23(a)). The gas content was 11–35 m^3/t at the end of this stage (Fig. 23(b)). Significantly, as shown in Fig. 23(a), this stage had stronger influence on the gas diffusion process. Influenced by differentiated uplifting, gases in the B1 block were drastically escaped while the gas escape in B2 block was relatively moderate (Fig. 23(a)). Besides, because the lower gas content retained in the early stage, the gas diffusion was weaker in B3 block during this stage. In terms of the B4 block, it had higher gas content after this stage (Fig. 23(b)) because of its lower escaping amount in stage IV and V.

During the last stage (65.5 Ma–now), the study area continued to be uplifted and eroded affected by the Himalayan tectonic movement, the CBM that preserved in the early stage was further diffused. At about 23 Ma, the fifth critical tectonic event caused a north-east to south-west compressive stress, which was nearly parallel to the axial direction of the reverse fault that formed in the early evolution stages. As a result of this stress field, the properties of some local thrust faults were reversed (e.g., some local thrust faults in the Puxian region) (Tian et al., 2012). Affected by the development of these open fault system, large quantities of gas were escaped. The gas saturation and gas content decreased rapidly in the east part of the study area (B2 domain, e.g. Well J25), while the gas diffusion in other areas (B1, B3, and B4) was relatively lower (Fig. 24(a), Table 2). In general, the combining effects of basin uplifting and tectonic inversion (the formation of extensional faults) controlled

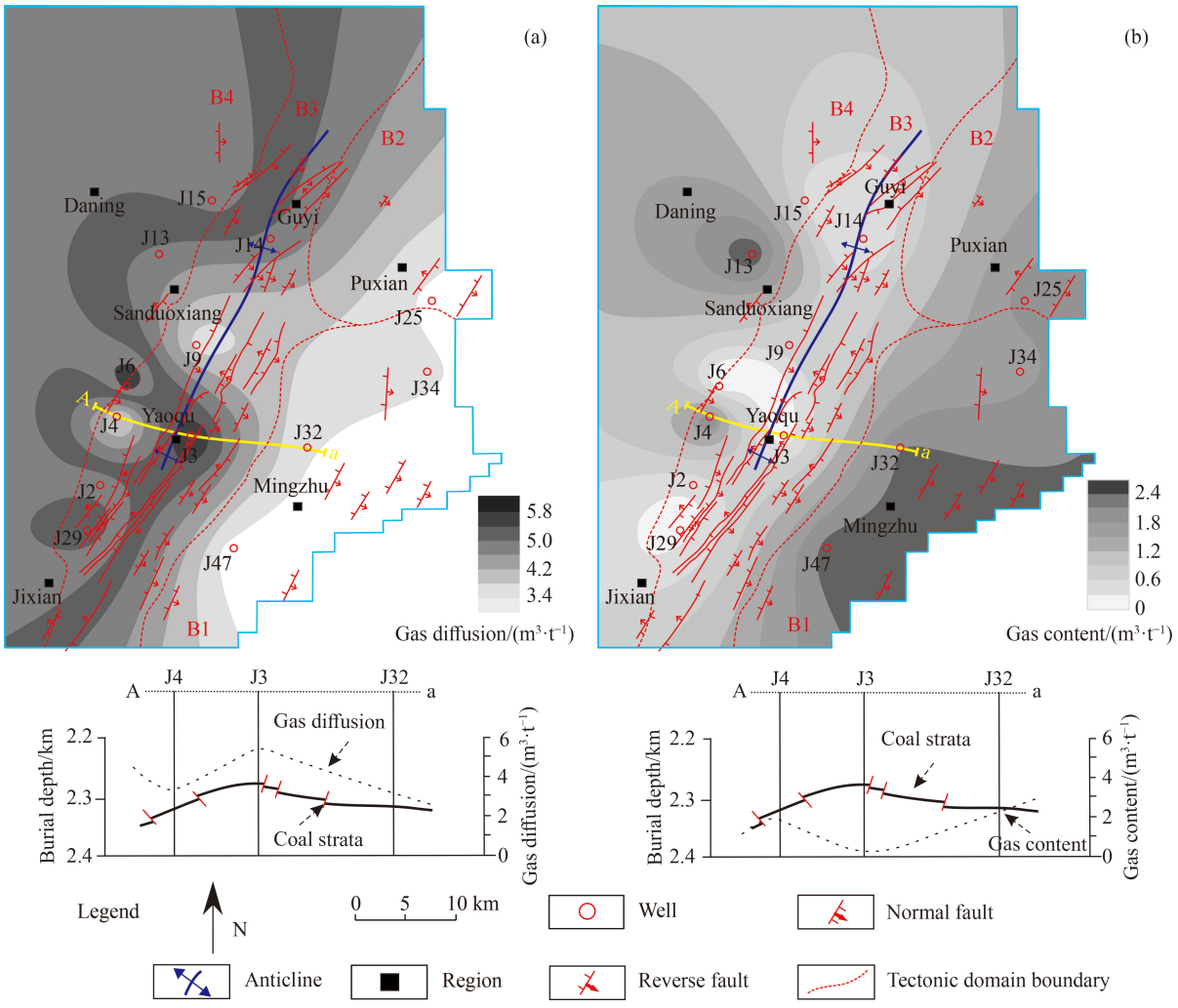

Fig. 21 Distribution characteristics of gas diffusion during the Jurassic (a) and gas content (b) at the end of the Late Jurassic.

the gas content and dissipation characteristics of reservoirs in this evolution period. The total amount of gas diffusion was about 1.5–15.5 m^3/t in this stage (Fig. 24(a)), and the current gas content was about 6–22 m^3/t in the whole region at the end of this stage (Fig. 24(b)).

Generally, the coal reservoir formation evolution process is a complex and continuous dynamic changing process, and multi-factors coupling effect finally leads to the distribution diversity of the current gas in coal reservoir. The distribution characteristics of CBM are controlled by hydrocarbon generation, gas preserved condition, buried depth, tectonic activities (i.e. experienced five critical tectonic events) and other geological conditions (e.g., hydrogeological characteristics) in each evolution stage.

5 Conclusions

In this paper, the tectonic subsidence history, geothermal field evolution history and methane accumulation features of Daning-Jixian block were studied by using numerical simulation. The main controlling factors of the current gas content heterogeneous distribution in the study area were clarified. The following three understandings have been formed.

1) The dynamic accumulation process of CBM is mainly controlled by three tectonic activities: the Indosinian Orogeny, the Yanshanian Orogeny and the Himalayan Orogeny.

2) The evolution of CBM reservoir can be divided into six stages: i. shallow-buried biogenic gas stage; ii. the primary thermogenic gas generation stage; iii. The turbulence uplifting and diffusion stage; iv. the secondary thermal gas generation stage; v. monolithic uplifting gas escape stage; vi. structural inversion and further CBM diffusion stage.

3) Five tectonic events were the main reason that controls the complex and continuous dynamic change process of CBM accumulation during different evolution periods, and led to the differential distribution of gas content. i. The first tectonic event (the Late Triassic) led

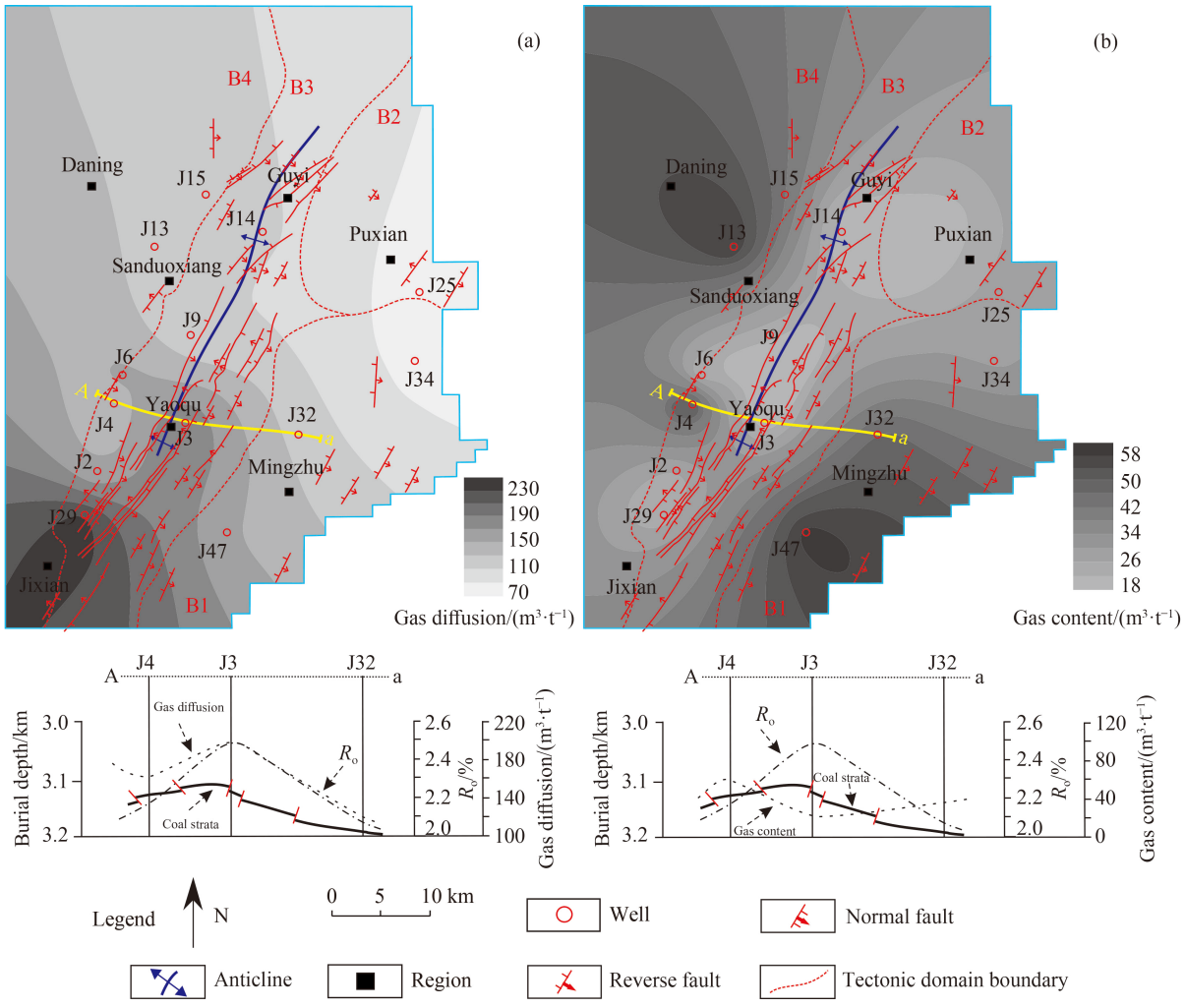

Fig. 22 Distribution characteristics of accumulative gas diffusion (a) and gas content (b) at the end of Early Cretaceous.

to the cessation of plutonic metamorphism and the dissipation of biogas and primary thermal gas that had been preserved during the early evolution stages. ii. The second tectonic event (the Middle and Late Jurassic) led to the differential escape of primary CBM, especially in B3 block. iii. The third tectonic event involved the Middle Yanshanian magma-heat events (the Early Cretaceous), which dominated the distribution of the secondary CBM generation and gas diffusion combing with the influence of an opening tectonic structural system. iv. The fourth tectonic event controlled differentiated uplifting (the Late Cretaceous) resulted in drastically escape of CBM in B1 block than other tectonic domains. v. The fifth tectonic event, the Neogene Himalayan structural inversion, caused the reversion of some local thrust faults and the low gas content in the B1 block.

Acknowledgments This research was funded by the National Natural Science Foundation of China (Grant No. 41902178), National Science and Technology Major Project (Oil & Gas) (No. 2016ZX05065), Natural Science Foundation of Shanxi Province, China (No. 20210302123165), Open Fund of Beijing Key Laboratory of Unconventional Natural Gas Geological Evaluation and Development Engineering, China University of Geosciences (Beijing) (No. 2019BJ02001).

References

Alsaab D, Elie M, Izart A, Sachsenhofer R F, Privalov V A, Suarez-Ruiz I, Martinez L, Panova E A (2009). Distribution of thermogenic methane in Carboniferous coal seams of the Donets Basin (Ukraine): “applications to exploitation of methane and forecast of mining hazards”. Int J Coal Geol, 78(1): 27–37

Boreham C J, Golding S D, Glikson M (1998). Factors controlling the origin of gas in Australian Bowen Basin coals. Org Geochem, 29(1–3): 347–362

Bustin A M M, Bustin R M (2008). Coal reservoir saturation: impact of temperature and pressure. AAPG Bull, 92(1): 77–86

Cai Y D, Liu D M, Yao Y B, Li J Q, Qiu Y K (2011). Geological controls on prediction of coalbed methane of No. 3 coal seam in Southern Qinshui Basin, north China. Int J Coal Geol, 88(2–3): 101–112

Cai Y D, Liu D M, Zhang K M, Elsworth D, Yao Y B, Tang D Z (2014). Preliminary evaluation of gas content of the No. 2 coal seam in the Yanchuannan area, southeast Ordos Basin, China. J Pet

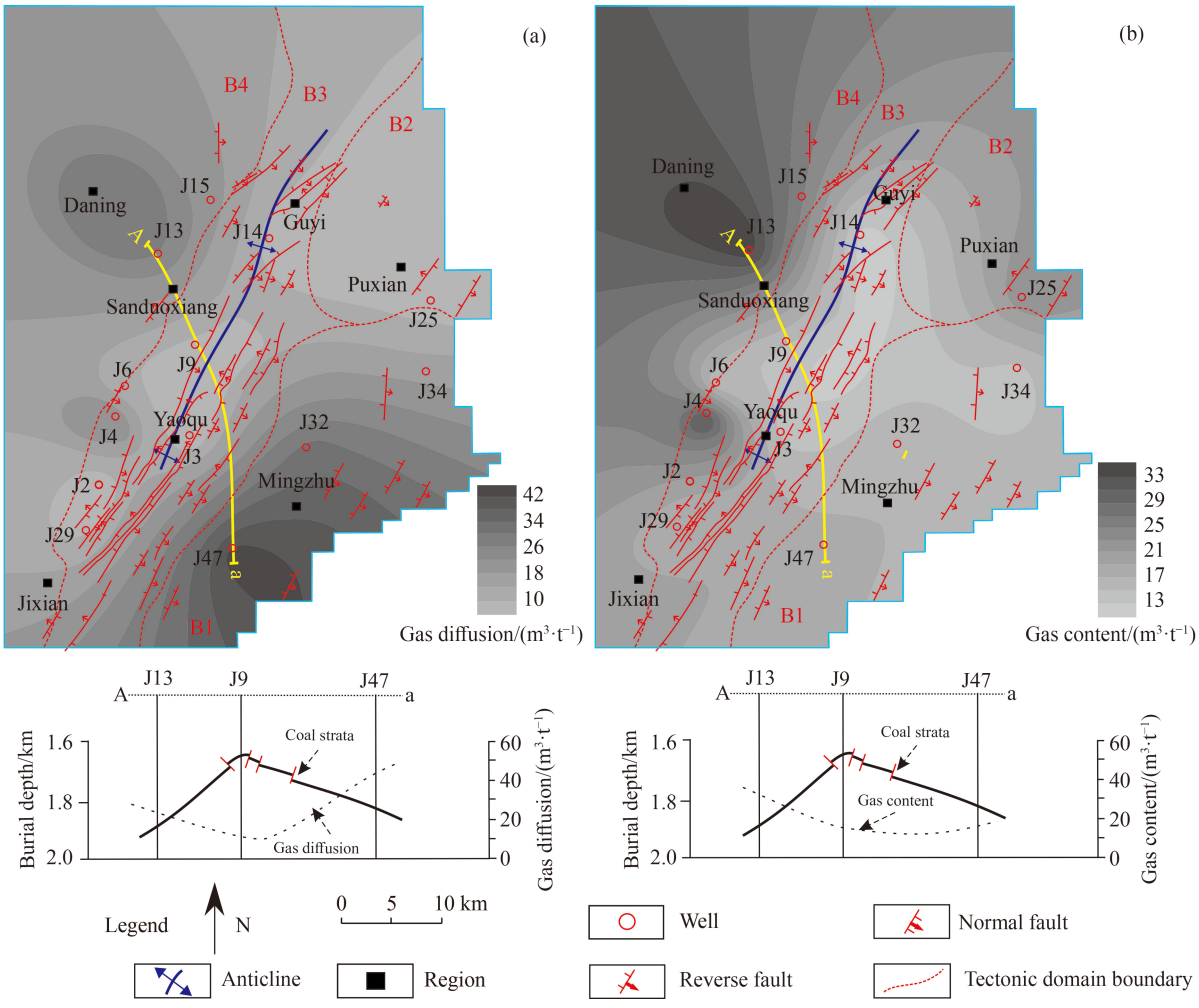

Fig. 23 Distribution characteristics of gas diffusion in stage V (a) and gas content at the end of Late Cretaceous (b).

Sci Eng, 122: 675–689

Cao D Y, Nie J, Wang A M, Zhang S R, Zhang B (2018). Structural and thermal control of enrichment conditions of coal measure gases in Linxing block of eastern Ordos Basin. J China Coal Soc, 43(6): 1526–1532 (in Chinese)

Chao H Y, Wang Y B (2016). Origin of coalbed methane and its influence in Linfen, southeastern Ordos Basin. J China Coal Soc, 41(7): 1769–1777 (in Chinese)

Faiz M, Saghafi A, Sherwood N, Wang I (2007). The influence of petrological properties and burial history on coal seam methane reservoir characterisation, Sydney Basin, Australia. Int J Coal Geol, 70: 193–208

Huang H X, Nie Z H, Chao H Y, Chen D, Zhao Z P, Liu Y (2018). Discussion of the selection for producing layers of deep CBM wells in Linfen Block. J China Coal Soc, 43(6): 1627–1633 (in Chinese)

Jiang B, Wang J L, Qu Z H, Li C G, Wang L L, Li M, Liu J G (2016). The stress characteristics of the Daning-Jixian area and its influence on the permeability of the coal reservoir. Earth Sci Front, 23(3): 17–23 (in Chinese)

Johnson R C, Flores R M (1998). Developmental geology of coalbed methane from shallow to deep in Rocky Mountain basins and in Cook Inlet-Matanuska basin, Alaska, U.S.A. and Canada. Int J Coal Geol, 35(1–4): 241–282

Karacan C O, Goodman G V R (2012). Analyses of geological and hydrodynamic controls on methane emissions experienced in a Lower Kittanning coal mine. Int J Coal Geol, 98: 110–127

Li S G, Wang C W, Wang H N, Wang Y B, Xu F Y, Guo Z D, Liu X W (2022). Reservoir forming characteristics and favorable area evaluation of deep coalbed methane in Daning-Jixian block. Coal Geo Explor 50(9): 59–67 (in Chinese)

Li W Z, Chen G, Sun B, Sun F J, Zhao Q B (2011). Geological controls of coalbed methane enrichment in Daning-Jixian area, southeastern Ordos Basin. Nat Gas Geosci, 22(2): 352–360 (in Chinese)

Li X Z, Wang Y H, Jiang Z C, Chen Z L, Wang L Z, Wu Q (2016). Progress and study on exploration and production for deep coalbed methane. J China Coal Soc, 41(1): 24–31 (in Chinese)

Mu X, Wang K, Yao X L (2016). Genesis analysis of CBM in Daning-Jixian region. China Coalbed Methane, 13(2): 26–30 (in Chinese)

Nie Z H, Chao H Y, Liu Y, Huang H X, Yu L Z (2018). Development strategy and production characteristics of deep coalbed methane in the east Ordos Basin: taking Daning-Jixian block for example. J China Coal Soc, 43(6): 1738–1746(in Chinese)

Nie Z H, Shi X S, Sun W, Yan X, Huang H X, Liu Y, Feng Y Q (2022). Production characteristics of deep coalbed methane gas reservoir in Daning-Jixian Block and its development technology

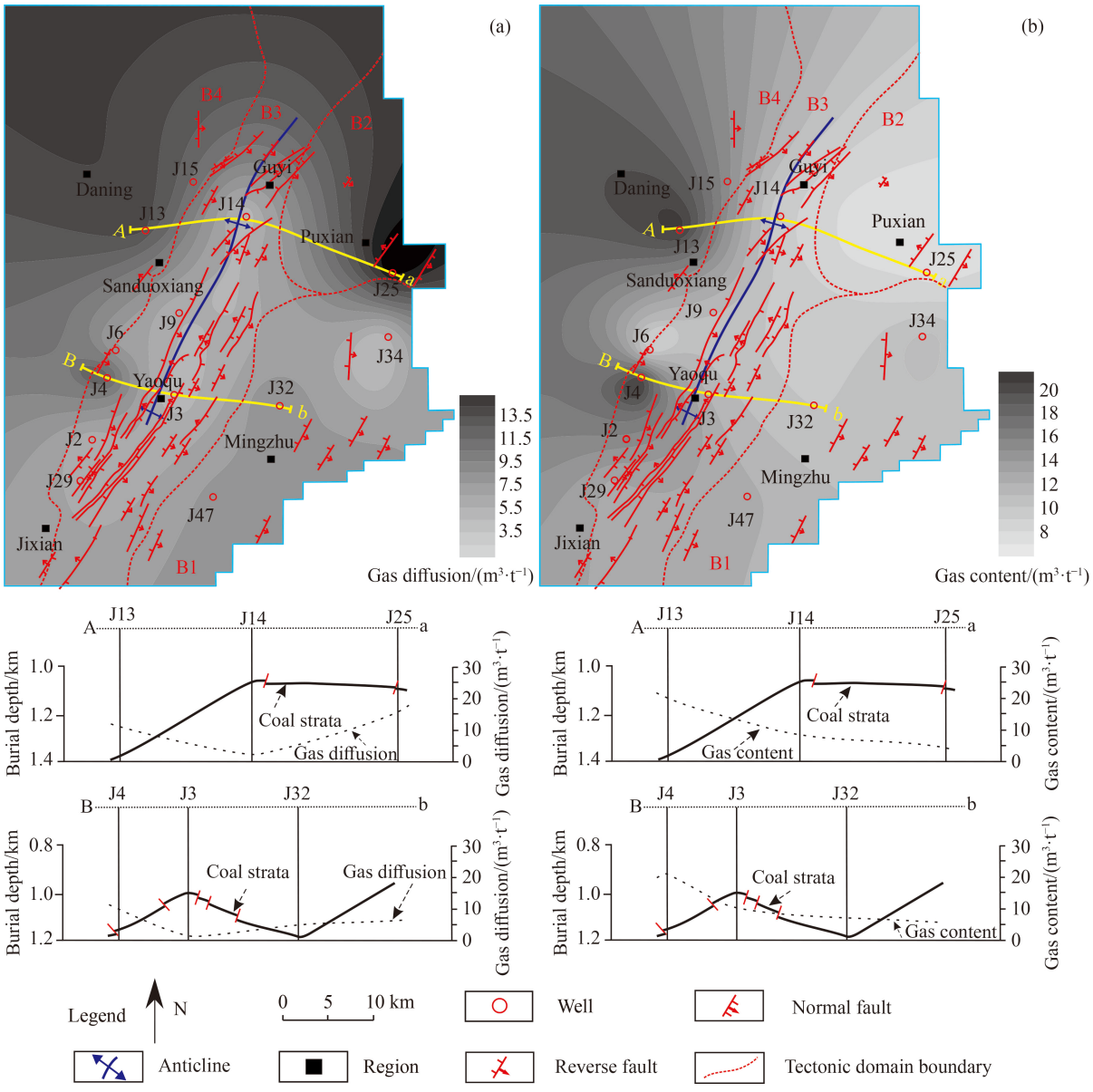

Fig. 24 Distribution characteristics of gas diffusion in the last evolution period (a) and current gas content (b).

countermeasures. Coal Geol Explor, 50(3): 193–200 (in Chinese)

Niu H Q (2010). The enriching and reservoiring laws of the coal bed methane in Ordos Basin. Dissertation for the Doctoral Degree. Qingdao: China University of Petroleum (in Chinese)

Payne D F, Ortoleva P J (2001). A model for lignin alteration-part II: numerical model of natural gas generation and application to the Piceance Basin, Western Colorado. Org Geochem, 32(9): 1087–1101

Qin Y, Shen J (2016). On the fundamental issues of deep coalbed methane geology. Acta Petrol Sin, 37(1): 125–136 (in Chinese)

Sachsenhofer R F, Privalov V A, Panova E A (2012). Basin evolution and coal geology of the Donets Basin (Ukraine, Russia): an overview. Int J Coal Geol, 89: 26–40

Scott AR, (2002). Hydrogeologic factors affecting gas content distribution in coal beds. Int J Coal Geol 50: 363–387

Scott A R, Kaiser W R, Ayers J W B (1994). Thermogenic and secondary biogenic gases, San Juan Basin, Colorado and New Mexicoe implications for coalbed methane producibility. AAPG Bull, 78(8): 1186–1209

Song Y, Liu H L, Hong F, Qin S F, Liu S B, Li G Z, Zhao M J (2012). Syncline reservoir pooling as a general model for coalbed methane (CBM) accumulations: mechanisms and case studies. J Petrol Sci Eng, 88–89: 5–12

Stauffer P H, Surdam R C, Jiao Z S, Miller T A, Bentley R D (2009). Combining geologic data and numerical modeling to improve estimates of the CO_2 sequestration potential of the Rock Springs Uplift, Wyoming. Energy Procedia, 1: 2717–2724

Sun B, Wang X H, Chen C H, Zhang J D (2004). Distribution characteristics of the coalbed methane at Daning-Jixian region in Ordos Basin. Nat Gas Ind, 24(5): 17–20 (in Chinese)

Sun Q P, Wang S W (2006). The deposit environment analysis of the coal bearing strata and its significance to the coalbed methane

development in Daning-Jixian region. Nat Gas Geosci, 17(6): 874–879 (in Chinese)

Tian W G (2012). CBM enrichment rules of eastern Ordos Basin and controlling mechanism. Dissertation for the Doctoral Degree. Beijing: China University of Geosciences (Beijing) (in Chinese)

Vishal V, Singh T N, Ranjith P G (2015). Influence of sorption time in CO_2-ECBM process in Indian coals using coupled numerical simulation. Fuel, 139: 51–58

Wang L L (2014). Evaluation of joint development heterogeneity of coal reservoir based on structural dynamics and its application: an example from Linfen, the eastern margin of the Ordos basin. Dissertation for the Doctoral Degree. Xuzhou: China University of Mining and Technology (in Chinese)

Wang L L, Jiang B, Qu Z H (2013). Structural control on gas content distribution in eastern margin of Ordos Basin. Coal Geol Explor, 41(1): 14–19 (in Chinese)

Wei C T, Qin Y, Jiang B, Fu X H, Zhang Z Q, Guo J (2008). Dynamic accumulation process of coalbed methane in residual basins of north China – a case study of the Qinshui Basin and the eastern margin of Ordos Basin. Acta Geol Sin, 82(10): 1363–1367 (in Chinese)

Wei C T, Qin Y, Wang G G X, Fu X H, Zhang Z Q (2010). Numerical simulation of coalbed methane generation, dissipation and retention in SE edge of Ordos Basin, China. Int J Coal Geol, 82: 147–159

Wei C T, Qin Y, Wang G X, Fu X H, Jiang B, Zhang Z Q (2007). Simulation study on evolution of coalbed methane reservoir in Qinshui basin, China. Int J Coal Geol, 72: 53–69

Wu C L, Yang Q, Zhu Z D, Liu G, Li X (2000). Thermodynamic analysis and simulation of coal metamorphism in the Fushun Basin, China. Int J Coal Geol, 44: 149–168

Xu H, Tang D Z, Tang S H, Zhang W Z, Meng Y J, Gao L J, Xie S Z, Zhao J L (2015). Geologic and hydrological controls on coal reservoir water production in marine coal-bearing strata: a case study of the Carboniferous Taiyuan Formation in the Liulin area, eastern Ordos Basin, China. Mar Pet Geol, 59: 517–526

Yan T T, He S, Bai Y D, He Z Y, Liu D M, Zeng F G, Chen X Z, Fu X Y (2021b). A study on the heterogeneity characteristics of geological controls on coalbed methane accumulation in Gujiao coalbed methane field, Xishan coalfield, China. Geofluids, 2021(1): 1–20

Yan T T, Yao Y B, Liu D M (2015). Critical tectonic events and their geological controls on gas generation, migration, and accumulation in the Weibei coalbed methane field, southeast Ordos basin. J Nat Gas Sci Eng, 27: 1367–1380

Yang X C, Qu Z H, Jiang B, Zhou K, Zhang J K (2013). Mesozoic-Cenozoic structural features and their evolution in Daning-Jixian area, Shanxi. Coal Geo China, 25(5): 1–6 (in Chinese)

Yan X, Xu F Y, Nie Z H, Kang Y S (2021a). Microstructure characteristics of Daji area in east Ordos Basin and its control over the high yield dessert of CBM. J China Coal Soc, 46(8): 2426–2439 (in Chinese)

Yao Y B, Liu D M, Tang D Z, Tang S H, Che Y, Huang W H (2009). Preliminary evaluation of the coalbed methane production potential and its geological controls in the Weibei Coalfield, Southeastern Ordos Basin, China. Int J Coal Geol, 78: 1–15